Truncated denitrifiers dominate the denitrification pathway in tundra soil metagenomes

Igor S. Pessi[1,2], Sirja Viitamäki[1], Anna-Maria Virkkala[3,4], Eeva Eronen-Rasimus[1,5], Tom O. Delmont[6], Maija E. Marushchak[7,8], Miska Luoto[3], and Jenni Hultman[1,2,9,*]

[1]Department of Microbiology, University of Helsinki, Helsinki, Finland
[2]Helsinki Institute of Sustainability Science (HELSUS), Helsinki, Finland
[3]Department of Geosciences and Geography, University of Helsinki, Helsinki, Finland
[4]Woodwell Climate Research Center, Falmouth, MA, USA
[5]Marine Research Centre, Finnish Environment Institute (SYKE), Helsinki, Finland
[6]Department of Bioinformatics, Genoscope, Paris, France
[7]Department of Biological and Environmental Science, University of Jyväskylä, Jyväskylä, Finland
[8]Department of Environmental and Biological Sciences, University of Eastern Finland, Kuopio, Finland
[9]Natural Resources Institute Finland (Luke), Helsinki, Finland
[*]Corresponding author: jenni.hultman@helsinki.fi

Abstract

In contrast to earlier assumptions, there is now mounting evidence for the role of tundra soils as important sources of the greenhouse gas nitrous oxide (N_2O). However, the microorganisms involved in the cycling of N_2O in this system remain largely uncharacterized. Since tundra soils are variable sources and sinks of N_2O we aimed to investigate the links between microbial community structure and N_2O cycling in this system. We analysed 1.4 Tb of metagenomic data and manually binned and curated 796 metagenome-assembled genomes (MAGs) from soils in northern Finland covering a range of ecosystems from dry upland soils to water-logged fens. We then searched for MAGs harbouring genes involved in denitrification, an important biotic process driving N_2O emissions. Communities of potential denitrifiers were dominated by microorganisms with truncated denitrification pathways (i.e. lacking one or more denitrification genes) and differed across soil ecosystems. Upland soils had a strong N_2O sink potential and were dominated by members of the Alphaproteobacteria such as *Bradyrhizobium* and *Reyranella*. Fens, which had in general net-zero N_2O fluxes, had a high abundance of poorly characterized taxa affiliated with the Chloroflexota lineage Ellin6529 and the Acidobacteriota subdivision Gp23. By coupling an in-depth characterization of microbial communities with *in situ* measurements of N_2O fluxes, our results suggest that the observed spatial patterns of N_2O cycling are driven by the composition of denitrifier communities.

Background

Nitrous oxide (N_2O) is a greenhouse gas (GHG) that has approximately 300 times the global warming potential of carbon dioxide on a 100-year scale [1]. Atmospheric N_2O concentrations have increased by nearly 20% since pre-industrial times, with soils – both natural and anthropogenic – accounting for up to 70% of the global emissions [2]. Despite being nitrogen (N) limited and enduring low temperatures throughout most of the year, tundra soils are increasingly recognized as important sources of N_2O [3–7]. The relative contribution of tundra soils to global GHG emissions is predicted to increase in the future [8, 9], as the warming rate at high latitude environments is more than twice as high than in other regions [10].

Microbial denitrification is an important biotic source of N_2O [11]. Denitrification is a series of enzymatic steps in which nitrate (NO_3^-) is sequentially reduced to nitrite (NO_2^-), nitric oxide (NO), N_2O, and dinitrogen (N_2) via the activity of the Nar, Nir, Nor, and Nos enzymes, respectively. The denitrification trait is common across a wide range of archaea, bacteria, and some fungi, most of which are facultative anaerobes that switch to N oxides as electron acceptor when oxygen becomes limiting [12]. Denitrification is a modular community process performed in synergy by different microbial taxa that execute only a subset of the complete denitrification pathway [12, 13]. With the growing number of microbial genomes sequenced in recent years, it has become evident that only a fraction of the microorganisms involved in the denitrification pathway encode the enzymatic machinery needed for complete denitrification [14, 15]. For instance, a study that investigated 652 genomes of cultured denitrifiers showed that approximately 31% encode the full set of enzymes needed for complete denitrification [14].

Modelling N_2O emissions based on microbial community structure is challenging. N_2O fluxes are characterized by a high temporal and spatial heterogeneity driven by several environmental constraints related to soil pH, N, moisture, and oxygen content [11]. In addition, our knowledge of the regulation of the denitrification process is largely based on the activity of model organisms such as the complete denitrifier *Paracoccus denitrificans* [16]. It has been suggested that incomplete denitrifiers that contain Nir and Nor but lack Nos contribute substantially to soil N_2O emissions [17], while non-denitrifying N_2O reducers, i.e. microorganisms that contain Nos but lack Nir, can represent an important N_2O sink [18–20]. Furthermore, the partitioning of metabolic pathways across different populations with truncated pathways – also known as metabolic handoffs [21] – has been linked to higher efficiencies in substrate consumption compared to complete pathways [15, 22]. However, it remains largely unclear how populations of truncated denitrifiers with different sets of denitrification genes interact with each other and the environment impacting N_2O emissions *in situ*.

Compared to high N_2O-emitting systems such as agricultural and tropical soils, our knowledge of denitrifier communities in tundra soils is limited. As denitrification leads to the loss of N to the atmosphere, it enhances the N-limited status of tundra systems thus impacting both microbial and plant communities [23, 24]. Investigations of denitrifier diversity in the tundra have been largely limited to gene-centric surveys using microarrays, amplicon sequencing, qPCR, and read-based metagenomics, which provide limited information on the taxonomic identity and genomic composition of community members. These studies have shown that denitrifier communities in the tundra are dominated by members of the phyla Proteobacteria, Actinobacteria, and Bacteroidetes, and that the potential for complete denitrification is usually present at the community level [25–29]. However, it is not known whether the complete denitrification potential occurs within discrete microbial populations or is widespread throughout populations of truncated denitrifiers lacking one or more denitrification genes. In addition, tundra soils encompass many different ecosystems, some of which are notorious N_2O sources (e.g. bare peat surfaces [3]). N_2O consumption is usually favoured in wetlands, where low NO_3^- availability due to anoxia promotes the reduction of N_2O to N_2 [30]. In upland soils, N_2O fluxes vary in both time and space. Strong N_2O sinks have been observed specially in sparsely vegetated upland soils [7], but the microbial processes underlying N_2O consumption in these systems are largely unknown [31]. Altogether, these large differences in N_2O fluxes across tundra ecosystems indicate differences in the structure of microbial communities, but a comprehensive understanding of the microorganisms driving N_2O cycles in tundra soils is lacking.

The paucity of in-depth knowledge on denitrifying communities in the tundra impairs our ability to model current and future N_2O fluxes from this biome. A better understanding of the ecological, metabolic, and functional traits of denitrifiers is thus critical for improving current models and mitigating N_2O emissions [32]. This invariably relies on the characterization of the so-called uncultured majority, i.e. microorganisms that have not been cultured to date but which comprise a high proportion of the microbial diversity in complex ecosystems [33, 34]. Genome-resolved metagenomics is a powerful tool to access the genomes of uncultured microorganisms and has provided important insights into carbon cycling processes in tundra soils [35–37]. However, this approach has not yet been applied to investigate the mechanisms driving N_2O cycling in the tundra. Here, we used genome-resolved metagenomics to investigate the diversity and metabolic capabilities of potential denitrifiers across different tundra soil ecosystems characterised by a high variability in net N_2O fluxes. Our aim was to elucidate the denitrification potential of microbial populations and explore the relationship between microbial community structure and patterns of N_2O fluxes in these ecosystems. For this, we

analysed 1.4 Tb of metagenomic data from 69 soil samples from an area of mountain tundra biome in Kilpisjärvi, northern Finland, and obtained 796 manually curated metagenome-assembled genomes (MAGs).

Methods

Study area and sampling for metagenomic analysis

The Saana Nature Reserve (69.04°N, 20.79°E) is located in Kilpisjärvi, northern Finland **(Suppl. Fig. S1a)**. The area is part of the mountain tundra biome and is characterized by a mean annual temperature of –1.9°C and annual precipitation of 487 mm [38]. Our study sites are distributed across Mount Saana and Mount Korkea-Jehkas and the valley in between **(Suppl. Fig. S1b)**, and include barren soils, heathlands (dominated by evergreen and deciduous shrubs), meadows (dominated by graminoids and forbs), and fens **(Suppl. Fig. S1c)**. In previous studies, we have established in the area a systematic fine-scale sampling of microclimate, soil conditions, and vegetation in topographically distinct environments [39–41]. Local variation in topography and soil properties creates a mosaic of habitats characterized by contrasting ecological conditions. This makes the study setting ideal to investigate species-environment relationships and ecosystem functioning in the tundra [41–43].

Sampling for metagenomic analysis was performed across 43 sites (barren soils, n = 2; heathlands, n = 18; meadows, n = 7; fens, n = 16) in July 2017 and July 2018, during the growing season in the northern hemisphere. Samples were obtained with a soil corer sterilized with 70% ethanol and, when possible, cores were split into organic and mineral samples using a sterilized spatula. In total, 41 organic and 28 mineral samples were obtained for metagenomic analysis **(Suppl. Table S1)**. Samples were transferred to a whirl-pack bag and immediately frozen in dry ice. Samples were transported frozen to the laboratory at the University of Helsinki and kept at –80°C until analyses.

Soil physicochemical characterization and *in situ* measurement of GHG fluxes

Soil physicochemical characterization was done using an extended set of 228 sites distributed across the study area. Soil pH, moisture, and soil organic matter (SOM) content were measured according to Finnish (SFS) and international (ISO) standards (SFS 300, ISO 10390, and SFS 3008). Carbon (C) and N content were measured using a Vario Micro Cube machine (Elementar, Langenselbold, Germany). *In situ* ecosystem-level N_2O and methane (CH_4) fluxes were measured from 101 sites using a static, non-steady state, non-flow-through system composed of a darkened acrylic chamber (20 cm diameter, 25 cm height) [4, 44]. Measurements were

134 conducted between 2nd July and 2nd August 2018, between 10 am and 5 pm. Simultaneous
135 measurement of GHG fluxes and sampling for metagenomic sequencing was not possible due to
136 limited resources and logistic constraints. At each site, five 25 mL gas samples were taken
137 during a 50-minute chamber closure and transferred to evacuated Exetainer vials (Labco,
138 Lampeter, UK). Gas samples were analysed using an Agilent 7890B gas chromatograph (Agilent
139 Technologies, Santa Clara, CA, USA) equipped with an autosampler (Gilson, Middleton, WI,
140 USA) and a flame ionization detector for CH_4 and an electron capture detector for N_2O. Gas
141 concentrations were calculated from the gas chromatograph peak areas based on standard
142 curves with a CH_4 concentration of 0–100 ppm and a N_2O concentration of 0–5000 ppb.
143 Differences in physicochemical composition and rates of GHG fluxes across soil ecosystems were
144 assessed using one-way analysis of variance (ANOVA) followed by Tukey's HSD test with the
145 *lm* and *TukeyHSD* functions in R v3.6.3 [45].

146 **Metagenome sequencing and processing of raw data**

147 Total DNA and RNA were co-extracted as previously described [41]. Briefly, extraction was
148 performed on 0.5 g of soil using a hexadecyltrimethyl ammonium bromide (CTAB), phenol-
149 chloroform, and bead-beating protocol. DNA was purified using the AllPrep DNA Mini Kit
150 (QIAGEN, Hilden, Germany) and quantified using the Qubit dsDNA BR Assay Kit
151 (ThermoFisher Scientific, Waltham, MA, USA). Library preparation for Illumina metagenome
152 sequencing was performed using the Nextera XT DNA Library Preparation Kit (Illumina, San
153 Diego, CA, USA). Metagenomes were obtained for 69 samples across two paired-end NextSeq
154 (132–170 bp) and one NovaSeq (2 x 151 bp) runs **(Suppl. Table S1)**. Two samples were
155 additionally sequenced with Nanopore MinION. For this, libraries were prepared using the
156 SQK-LSK109 Ligation Sequencing Kit with the long fragment buffer (Oxford Nanopore
157 Technologies, Oxford, UK) and the NEBNext Companion Module for Oxford Nanopore
158 Technologies Ligation Sequencing Kit (New England Biolabs). Each sample was sequenced for
159 48 hours on one R9.4 flow cell.

160 The quality of the raw Illumina data was verified with fastQC v0.11.9 [46] and multiQC v1.8
161 [47]. Cutadapt v1.16 [48] was then used to trim sequencing adapters and low-quality base calls
162 ($q < 20$) and to filter out short reads (< 50 bp). Nanopore data were basecalled with GPU guppy
163 v4.0.11 using the high-accuracy model and applying a minimum quality score of 7. The quality
164 of the basecalled Nanopore data was assessed with pycoQC v2.5.0.21 [49] and adapters were
165 trimmed with Porechop v0.2.4 [50].

Taxonomic profiling

Taxonomic profiles of the microbial communities were obtained using a read-based approach, i.e. based on unassembled Illumina data. Due to differences in sequencing depth across the samples, the dataset was resampled to 2,000,000 reads per sample with seqtk v1.3 [51]. Reads matching the SSU rRNA gene were identified with METAXA v2.2 [52] and classified against the SILVA database release 138.1 [53] in mothur v1.44.3 [54] using the Wang's Naïve Bayesian Classifier [55] and a 80% confidence cut-off. Differences in community structure were assessed using non-metric multidimensional scaling (NMDS) and permutational ANOVA (PERMANOVA) with the package vegan v2.5.6 [56] in R v3.6.3 [45] (functions *metaMDS* and *adonis*, respectively).

Metagenome assembling and binning

Metagenome assembling of the Illumina data was performed as two co-assemblies. One co-assembly comprised the upland soils (barren, heathland, and meadow; n = 47) and the other the fen samples (n = 22). For each co-assembly, reads from the respective samples were pooled and assembled with MEGAHIT v1.1.1.2 [57]. Assembling of the Nanopore data was done for each sample individually with metaFlye v2.7.1 [58], and contigs were corrected based on Illumina data from the respective sample with bowtie v2.3.5 [59], SAMtools v1.9 [60], and pilon v1.23 [61]. Quality assessment of the (co-)assemblies was obtained with metaQUAST v5.0.2 [62].

MAG binning was done separately for each Illumina and Nanopore (co-)assembly with anvi'o v6.2 [63] after discarding contigs shorter than 2500 bp. Gene calls were predicted with prodigal v2.6.3 [64]. Single-copy genes were identified with HMMER v.3.2.1 [65] and classified with DIAMOND v0.9.14 [66] against the Genome Taxonomy Database (GTDB) release 04-RS89 [67, 68]. Illumina reads were mapped to the contigs with bowtie v2.3.5 [59] and SAM files were sorted and indexed using SAMtools v1.9 [60]. Due to their large sizes, Illumina co-assemblies were split into 100 smaller clusters based on differential coverage and tetranucleotide frequency with CONCOCT v1.0.0 [69]. Contigs were then manually sorted into bins based on the same composition and coverage metrics using the *anvi-interactive* interface in anvi'o v6.2 [63]. Nanopore contigs were binned directly without pre-clustering. Bins that were ≥ 50% complete according to the presence of single-copy genes were further refined using the *anvi-refine* interface in anvi'o v6.2 [63]. In addition to taxonomic signal (based on single-copy genes classified against GTDB), either differential coverage or tetranucleotide frequency was used to identify and remove outlying contigs. The former was used for bins with a large variation in contig coverage across samples, and the latter for those with marked differences in GC content

199 across contigs. Bins ≥ 50% complete and ≤ 10% redundant – hereafter referred as MAGs – were
200 kept for downstream analyses.

201 Gene-centric analyses

202 Functional profiles of the microbial communities were obtained using a gene-centric approach
203 based on assembled data. For each (co-)assembly, gene calls were translated to amino acid
204 sequences and searched against the KOfam hidden Markov model (HMM) database with
205 KofamScan v1.3.0 [70]. Only matches with scores above the pre-computed family-specific
206 thresholds were kept. Genes putatively identified as denitrification genes (*nirK*, *nirS*, *norB*, and
207 *nosZ*) were submitted to further analyses. Amino acid sequences were aligned with MAFFT
208 v7.429 [71] and alignments were visualized with Unipro UGENE v38.1 [72]. Sequences were
209 then inspected for the presence of conserved residues at the following positions: *nirK*, Cu-
210 binding and active sites [73]; *nirS*, c-heme and d_1-heme binding sites [74]; *norB*, binding of the
211 catalytic centres cyt b, b_3, and Fe_b [75]; *nosZ*: binding of the Cu_Z and Cu_A centres [75]. Sequences
212 which did not contain the correct amino acid at these positions were removed. Finally, resulting
213 amino acid sequences were aligned with MAFFT v7.429 [71] along with reference sequences
214 from Graf et al. [14] and a maximum-likelihood tree was computed with FastTree v2.1.11 [76]
215 using the LG+GAMMA model. Annotation of denitrification genes was also performed for
216 previously published genomes retrieved from GenBank. These included a set of 1529 MAGs
217 obtained from soils in Stordalen Mire, northern Sweden [37], and all (n = 69) genomes of
218 Acidobacteriota strains and candidate taxa (accessed on 9 October 2020).

219 The abundance of functional genes was computed based on read coverage with CoverM v0.6.1
220 [77]. For this, Illumina reads were mapped to the contigs with minimap v2.17 [78] and coverage
221 was normalized to reads per kilobase million (RPKM). Differences in functional community
222 structure were assessed using NMDS and PERMANOVA as described above for the taxonomic
223 profiles. Differences in the abundance of individual genes across soil ecosystems were assessed
224 using ANOVA followed by Tukey's HSD test with the *lm* and *TukeyHSD* functions in R v3.6.3
225 [45]. Relationships between the abundance of denitrification genes and N_2O flux rates were
226 assessed using linear regression in R v3.6.3 [45].

227 Phylogenomic analyses of MAGs and metabolic reconstruction

228 Phylogenetic placement of MAGs was done based on 122 archaeal and 120 bacterial single-copy
229 genes with GTDB-Tk v1.3.0 [79] and the GTDB release 05-RS95 [67, 68]. Acidobacteriota MAGs
230 containing denitrification genes were submitted to further phylogenomic analyses alongside all
231 genomes of Acidobacteriota strains and candidate taxa available on GenBank (n = 69; accessed

232 on 9 October 2020). For this, the amino acid sequence of 23 ribosomal proteins was retrieved for
233 each genome with anvi'o v6.2 [63] and aligned with MUSCLE v3.8.1551 [80]. A maximum
234 likelihood tree was then computed based on the concatenated alignments with FastTree v2.1.11
235 using the LG+GAMMA model [76]. *Escherichia coli* ATCC 11775 was used to root the tree.

236 For metabolic reconstruction, MAGs were annotated against the KOfam HMM database [70]
237 with HMMER v.3.2.1 [65] using the pre-computed score thresholds of each HMM profile. The
238 *anvi-estimate-metabolism* program in anvi'o v6.2 [63] was then used to predict the metabolic
239 capabilities of the MAGs. A metabolic pathway was considered present in MAGs containing at
240 least 75% of the genes involved in the pathway. Carbohydrate-active enzymes (CAZymes) were
241 annotated with dbCAN v.2.0 based on the dbCAN v7 HMM database [81]. Only hits with an e-
242 value < 1×10^{-14} and coverage > 0.35 were considered.

243 MAG dereplication and read recruitment analysis

244 Prior to read recruitment analyses, Illumina and Nanopore MAGs were dereplicated based on
245 a 99% average nucleotide identity (ANI) threshold with fastANI v1.3 [82] to remove redundancy
246 (i.e. MAGs that were recovered multiple times across the different assemblies). Read
247 recruitment analyses were then then performed with CoverM v0.6.1 [77]. For this, Illumina
248 reads were mapped to the set of non-redundant MAGs with minimap v2.17 [78] and relative
249 abundances were calculated as a proportion of the reads mapping to each MAG.

250 Results

251 Environmental characterization and *in situ* GHG fluxes

252 Our sampling design in Kilpisjärvi included two soil depths across four ecosystems that are
253 characteristic of the tundra biome (barren soils, heathlands, meadows, and fens) **(Suppl.**
254 **Figure S1a–c)**. Soil ecosystems differed in vegetation cover and physicochemical composition,
255 with fens in particular being characterized by higher pH, moisture, and N content (one-way
256 ANOVA, $R^2 = 0.16–0.64$, $p < 0.001$) and, together with the meadows, lower C:N ratio (one-way
257 ANOVA, $R^2 = 0.49$, $p < 0.001$) **(Suppl. Fig. S1d)**. *In situ* measurements of GHG fluxes showed
258 a high sink-source variability in net N_2O fluxes across the ecosystems **(Suppl. Fig. S1e)**.
259 Although the average N_2O flux across all sites was small (net consumption of
260 6 µg N_2O m^{-2} day^{-1}), high N_2O emission at rates of up to 660 µg N_2O m^{-2} day^{-1} was observed at
261 the meadow sites. Likewise, strong N_2O consumption (up to –435 µg N_2O m^{-2} day^{-1}) was
262 observed particularly at the heathland and meadow sites. Net CH_4 emissions were observed
263 exclusively at the fen sites **(Suppl. Fig. S1e)**.

Differences in microbial community structure across soils ecosystems

We obtained more than 9 billion Illumina (1.4 Tb) and 7 million Nanopore (21.5 Gb) reads from the 69 soil metagenomes (mean: 19.9 Gb, minimum: 0.7 Gb, maximum: 82.9 Gb) **(Suppl. Table S1)**. Two Illumina co-assemblies and two individual Nanopore assemblies yielded more than 4 million contigs longer than 2,500 bp, with a total assembly size of 21.1 Gb. The co-assemblies covered a significant fraction of the original metagenomic data, with an average read recruitment rate of 54.6% across samples (minimum: 22.9%, maximum: 75.8%).

Read-based analyses of unassembled SSU rRNA gene sequences showed that microbial community composition differed across the ecosystems, with fen soils harbouring contrasting microbial communities compared to the other ecosystems (PERMANOVA, $R^2 = 0.35$, $p < 0.001$) **(Suppl. Fig. S2a)**. No differences in community structure were observed between soil depths or the interaction between soil ecosystem and depth (PERMANOVA, $p > 0.05$). Among previously described (i.e. not unclassified) taxa, microbial communities in barren, heathland, and meadow soils were dominated by aerobic and facultative anaerobic heterotrophs such as *Acidipila*/*Silvibacterium*, *Bryobacter*, *Granulicella*, *Acidothermus*, *Conexibacter*, *Mycobacterium*, *Mucilaginibacter*, *Bradyrhizobium*, and *Roseiarcus* **(Suppl. Fig. S2b)**. On the other hand, fen soils were dominated by methanogenic archaea from the genera *Methanobacterium* and *Methanosaeta* and anaerobic bacteria such as *Thermoanaerobaculum*, *Desulfobacca*, and *Smithella*, but also the putative aerobic heterotroph *Candidatus* Koribacter.

Communities from different ecosystems also differed in their functional potential **(Suppl. Fig. S2c).** Denitrification genes (*nirK*, *nirS*, *norB*, and *nosZ*) were in general more abundant in the meadows and fens (one-way ANOVA, $R^2 = 0.48–0.76$, $p < 0.001$) **(Suppl. Fig. S2d)**. These were annotated using a three-step approach to avoid false positives consisting of distantly related homologues that are not involved in denitrification. Putative genes were first identified by searching predicted amino acid sequences against curated HMMs from the KOfam database [70]. Positive matches were then aligned and manually inspected for the presence of conserved residues at specific positions associated with the binding of co-factors and active sites [73–75]. Sequences containing the correct amino acid at these core positions were further submitted to phylogenetic analyses along with sequences from a comprehensive database of archaeal and bacterial genomes [14]. In addition to denitrification genes, fen soils also had a higher abundance of genes involved in sulfate reduction (*dsrA* and *dsrB*) and methanogenesis (*mcrA* and *mcrB)* (one-way ANOVA, $R^2 = 0.59–0.90$, $p < 0.001$). We did not observe a significant relationship between N_2O flux rates and neither the abundance of individual denitrification genes nor the ratio between *nosZ* and *nirK*+*nirS* abundances (linear regression, $p > 0.05$).

298 However, the ratio between *nosZ* and *nirK*+*nirS* abundances was higher in the meadows (one-
299 way ANOVA, $R^2 = 0.29$, $p < 0.001$) **(Suppl. Fig. S2d)**, which indicates a higher potential for
300 N_2O consumption in this ecosystem.

301 A manually curated genomic database from tundra soil metagenomes

302 Using anvi'o [63], we obtained 8,043 genomic bins and manually curated these to a set of 796
303 MAGs that were at least 50% complete and no more than 10% redundant **(Fig. 1, Suppl. Table**
304 **S2)**. According to estimates based on domain-specific single-copy genes, the obtained MAGs
305 were on average 65.4% complete (minimum: 50.0%, maximum: 100.0%) and 2.7% redundant
306 (minimum: 0.0%, maximum: 9.9%) **(Suppl. Table S2)**. Phylogenomic analyses based on 122
307 archaeal and 120 bacterial single-copy genes placed the MAGs across 35 bacterial and archaeal
308 phyla according to the GTDB classification [67, 68] **(Fig. 1).** The most represented phyla were
309 Acidobacteriota (n = 172), Actinobacteriota (n = 163), Proteobacteria (Alphaproteobacteria,
310 n = 54; Gammaproteobacteria, n = 39), Chloroflexota (n = 84), and Verrucomicrobiota (n = 43).
311 Most MAGs (n = 703) belonged to genera that do not comprise formally described species,
312 including 303 MAGs that were placed outside genus-level lineages currently described in GTDB
313 and thus likely represent novel genera **(Suppl. Table S2)**.

314 To investigate their distribution across the different soil ecosystems, MAGs were dereplicated
315 based on a 90% ANI threshold, yielding a set of 761 non-redundant MAGs **(Fig. 2)**. On average,
316 15.8% of the reads from each sample were recruited by the set of non-redundant MAGs
317 (minimum: 7.6%, maximum: 30.5%). In agreement with the read-based assessment, we
318 observed differences in MAG composition across the soil ecosystems, with only 50 MAGs shared
319 between the heathland, meadow, and fen soils **(Suppl. Fig. S3a)**. Fen soils harboured the
320 highest number of MAGs, with an average of 155 MAGs per sample **(Suppl. Fig. S3b)**.
321 Although barren and fen soils had similar taxonomic richness according to the read-based
322 estimates, only a small number of MAGs was detected in the barren soils (average of four MAGs
323 per sample). This is likely a result of limited sampling and sequencing of this ecosystem, which
324 consisted of four samples and a total of 7.9 Gb of metagenomic data **(Suppl. Table S1)**. The
325 number of MAGs in heathland and meadow soils was similar (average of 47 and 63 MAGs per
326 sample, respectively) **(Suppl. Fig. S3b)**. In general, barren, heathland, and meadow soils were
327 dominated by the same set of MAGs **(Suppl. Fig. S3c**). These included members of the
328 Acidobacteriota (*Sulfotelmatobacter* and unclassified genera in the class Acidobacteriae),
329 Actinobacteriota (*Mycobacterium* and unclassified genera in the family Streptosporangiaceae),
330 and Proteobacteria (Alphaproteobacteria: *Reyranella*, *Bradyrhizobium*, and unclassified
331 Xanthobacteraceae; Gammaproteobacteria: unclassified Steroidobacteraceae). On the other

hand, fen soils were dominated by MAGs that were not assigned to formally described genera, including lineages of Acidobacteriota (family Koribacteraceae), Actinobacteriota (family Solirubrobacteraceae), Chloroflexota (class Ellin6529), Desulfobacterota (order Desulfobaccales), and Halobacterota.

Fig. 1 | Genome-resolved metagenomics of tundra soils. Phylogenomic placement and assembly statistics of 796 metagenome-assembled genomes (MAGs) recovered from soils in Kilpisjärvi, northern Finland. Unrooted maximum likelihood tree based on concatenated alignments of amino acid sequences from 122 archaeal and 120 bacterial single-copy genes. Additional information about the MAGs can be found in **Suppl. Table S2**.

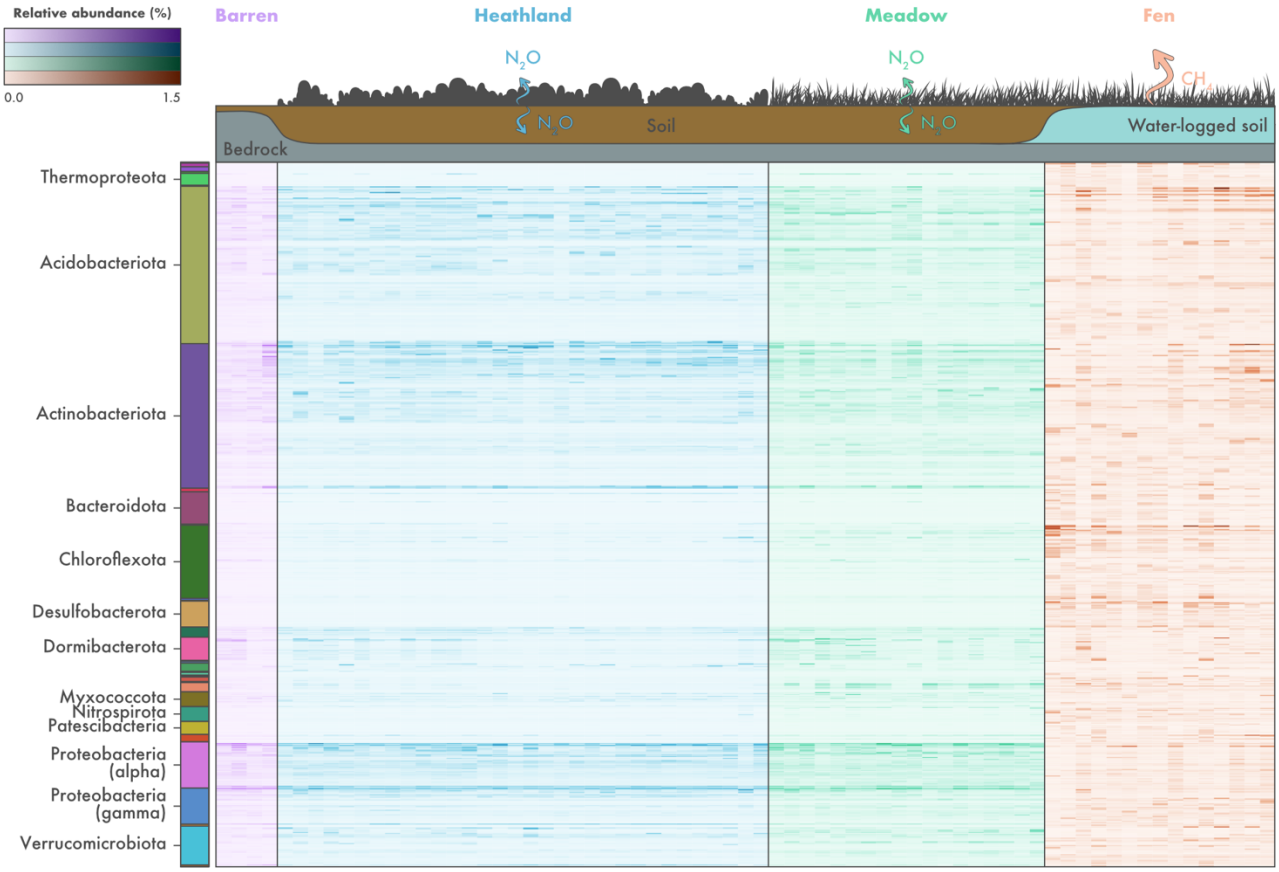

Fig. 2 | Microbial community composition across different soil ecosystems in the tundra. Relative abundance of 761 non-redundant metagenome-assembled genomes (MAGs) recovered from soils in Kilpisjärvi, northern Finland. Relative abundances were computed as a proportion of the reads mapping to each MAG. Phylum-level taxonomic assignments are shown for the major groups found. The scheme on the top of the figure represents ecosystem-level methane (CH_4) and nitrous oxide (N_2O) fluxes based on *in situ* measurements **(Suppl. Fig. S1)**.

Microorganisms from tundra soils have truncated denitrification pathways

To gain insights into the microorganisms involved with the cycling of N_2O in tundra soils, we traced the curated denitrification genes to the set of recovered MAGs. Denitrification genes were found in 110 of the 796 MAGs (13.8%) **(Suppl. Table S2)**. These were affiliated with the archaeal phylum Thermoproteota and many bacterial phyla such as Proteobacteria (Gamma- and Alphaproteobacteria), Acidobacteriota, Bacteroidota, Actinobacteriota, Chloroflexota, and Verrucomicrobiota **(Fig. 3a)**. However, only 17 MAGs were assigned to a validly described genera **(Suppl. Table S2)**. These included members of the Acidobacteriota (*Solibacter*, *Sulfotelmatobacter*, *Terracidiphilus*, and *Gaiella*), Myxococcota (*Anaeromyxobacter*), Planctomycetota (*Singulisphaera*), Proteobacteria (Alphaproteobacteria: *Bauldia*, *Bradyrhizobium*, *Methylocella*, and *Reyranella*; Gammaproteobacteria: *Gallionella* and

358 *Rhizobacter*), and Verrucomicrobiota (*Lacunisphaera* and *Opitutus*). On average, 1.8% of the
359 reads in each sample were recruited by all denitrifiers combined (minimum: 0.4%, maximum:
360 6.1%).

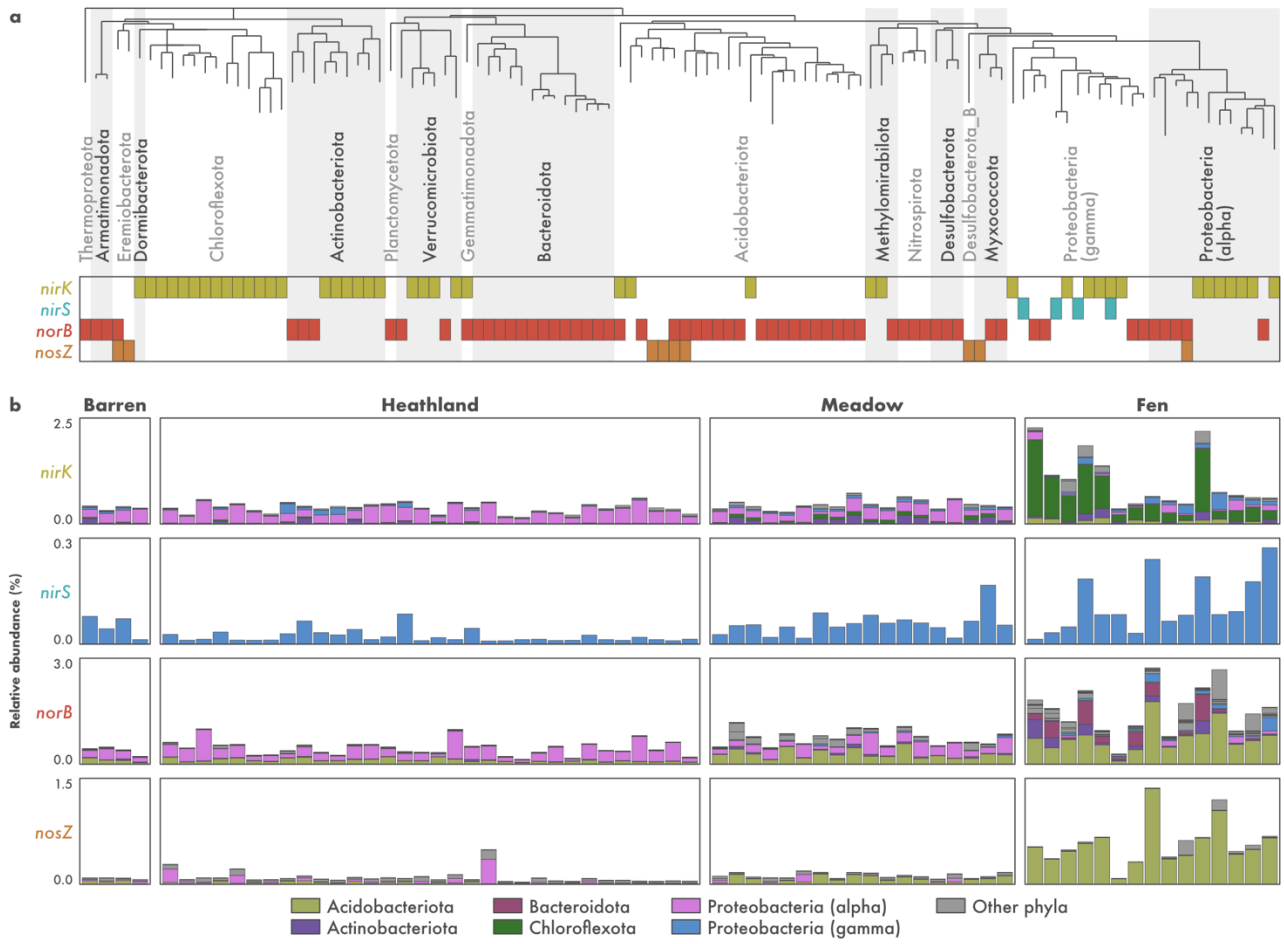

361 **Fig. 3 | Metabolic potential for denitrification in tundra soils. a)** Distribution of
362 denitrification genes across 110 metagenome-assembled genomes (MAGs) recovered from
363 tundra soils in Kilpisjärvi, northern Finland. Genes encoding the nitrite (*nirK*/*nirS*), nitric oxide
364 (*norB*), and nitrous oxide (*nosZ*) reductases were annotated using a three-step approach
365 including (1) identification using hidden Markov models from the KOfam database, (2) manual
366 inspection for the presence of conserved residues at positions associated with the binding of co-
367 factors and active sites, and (3) phylogenetic analyses along with sequences from archaeal and
368 bacterial genomes **(Suppl. Fig. S5)**. **b)** Phylum-level relative abundance of microorganisms
369 harbouring denitrification genes across the different soil ecosystems, computed as a proportion
370 of reads mapping to each MAG.

371 Genes involved in denitrification were found exclusively in MAGs with truncated denitrification
372 pathways, i.e. MAGs missing one or more genes involved in the complete denitrification process

373 **(Fig. 3a)**. Of the 110 MAGs harbouring denitrification genes, the vast majority (n = 104)
374 encoded only one of the Nir, Nor, and Nos enzymes and no MAG encoded all the three enzymes
375 required for the reduction of NO_2^- to N_2. Unsurprisingly, co-occurrence of genes encoding the
376 three enzymes was also not observed in any of the other genomic bins of lower quality that were
377 discarded from the final MAG dataset (i.e. bins that were < 50% complete and/or > 10%
378 redundant). To verify if microorganisms with truncated denitrification pathways are common
379 in other tundra systems, we expanded our analysis to 1529 MAGs recovered from permafrost
380 peatland, bog, and fen soils in Stordalen Mire, northern Sweden [37]. Among these, 225 MAGs
381 (14.7%) contained denitrification genes **(Suppl. Fig. S4)**. MAGs encompassed a similar
382 taxonomic profile as observed in the Kilpisjärvi dataset, and MAGs with truncated
383 denitrification pathways were also the norm in Stordalen Mire soils. Only one MAG, assigned
384 to the Gammaproteobacteria genus *Janthinobacterium*, encoded all the Nir, Nor, and Nos
385 enzymes required for the reduction of NO_2^- to N_2.

386 Microorganisms affiliated with the Chloroflexota lineage Ellin6529 are the 387 main denitrifiers *stricto sensu* in fen soils

388 The reduction of NO_2^- to NO, performed by microorganisms harbouring the *nirK* or *nirS* genes,
389 is the hallmark step of denitrification and is often referred to as denitrification *stricto sensu* as
390 it involves the conversion of a soluble substrate to a gaseous product thus leading to the removal
391 of N from the system [12]. Of the 110 Kilpisjärvi MAGs harbouring genes involved in
392 denitrification, 46 contained *nirK*/*nirS* genes and are thus potential denitrifiers *stricto sensu*
393 **(Fig. 3a)**. These belonged mainly to the bacterial phyla Chloroflexota, Actinobacteriota, and
394 Proteobacteria (Alpha- and Gammaproteobacteria). Most MAGs (n = 43) contained the *nirK*
395 gene, which encodes the copper-containing form of Nir **(Suppl. Fig. S5a)**. The *nirS* gene
396 encoding the cytochrome cd_1-containing form of Nir was present in four Gammaproteobacteria
397 MAGs **(Suppl. Fig. S5b)**, including one MAG that contained both genes.

398 The composition of potential denitrifier *stricto sensu* communities differed across the ecosystems
399 **(Fig. 3b)**. MAGs belonging to the Alphaproteobacteria class of the Proteobacteria were the most
400 abundant in the barren, heathland, and meadow soils, particularly the MAG KUL-0154
401 assigned to the genera *Bradyrhizobium* **(Suppl. Fig. S6)**. Two other Alphaproteobacteria
402 MAGs that do not correspond to formally described genera in the families Acetobacteraceae and
403 Beijerinckiaceae (KUL-0057 and KUL-0056, respectively) were also found at high abundances.
404 In addition, one Actinobacteriota MAG assigned to an uncharacterized genus in the family
405 Gaiellaceae (KWL-0073), was abundant in the meadow soils. On the other hand, fen

406 communities were dominated by MAGs belonging to the phylum Chloroflexota **(Fig. 3b)**, which
407 included seven MAGs assigned to the class-level lineage Ellin6529 **(Suppl. Fig. S6)**.

408 None of the Ellin6529 MAGs contained the key genes involved in autotrophic carbon fixation,
409 dissimilatory sulfate reduction, dissimilatory nitrate reduction to ammonia, and nitrogen
410 fixation **(Suppl. Table S3)**. Analysis of genes encoding terminal oxidases involved in the
411 aerobic respiratory electron chain revealed that all seven Ellin6529 MAGs harboured the
412 *coxABC* genes encoding the *aa3*-type cytochrome c oxidase**.** Four MAGs also contained the
413 *cydAB* genes encoding the cytochrome *bd* ubiquinol oxidase, a terminal oxidase with high
414 affinity for oxygen that also plays a role in preventing the inactivation of oxygen-sensitive
415 enzymes and protecting against oxidative and nitrosative stress, toxic compounds such as
416 cyanide, and other stress conditions such as high temperature and high pH [83, 84]. The
417 dominant MAGs in the barren, heathland, and meadow soils encoded a different set of aerobic
418 terminal oxidases. In addition to the *cydAB* genes, the MAGs KUL-0057 and KUL-0154 also
419 contained the *cyoABCD* genes encoding the cytochrome o ubiquinol oxidase, which is the main
420 terminal oxidase under highly aerobic conditions [85], and KUL-0057 also contained genes
421 encoding the *cbb3*-type cytochrome c oxidase, a terminal oxidase with high affinity for oxygen
422 [86]. Genes involved in the Calvin cycle (e.g. *rbcL*, *rbcS*, and *prkB*) were found in the
423 *Bradyrhizobium* MAG (KUL-0154), and none of the key genes for autotrophic carbon fixation
424 pathways were present in the other dominant Alphaproteobacteria MAGs.

425 Acidobacteriota with the potential to reduce NO and N_2O are abundant in the fens

426 The stepwise reduction of NO to N_2O and N_2 carried out by microorganisms containing the *norB*
427 and *nosZ* genes, respectively, represents the final step of denitrification and the main biotic
428 control on N_2O emissions. Soil denitrification rates depend on multiple environmental
429 conditions such as adequate moisture and inorganic N availability, but whether it results in the
430 emission of N_2O or N_2 is ultimately linked to a balance between the activity of NO and N_2O
431 reducers [11, 15]. *norB* and *nosZ* genes were identified in 62 and 9 Kilpisjärvi MAGs,
432 respectively, belonging mostly to the phyla Actinobacteriota, Bacteroidota, Acidobacteriota, and
433 Proteobacteria (class Alphaproteobacteria) **(Fig. 3a)**. With the exception of one
434 Gemmatimonadota and one Acidobacteriota MAG, *norB*- and *nosZ*-containing MAGs were
435 almost exclusively non-denitrifiers *stricto sensu*, i.e. they did not harbour the *nirK*/*nirS* genes
436 involved in the reduction of NO_2^- to NO. Most MAGs (n = 48) harboured a *norB* gene encoding
437 the monomeric, quinol-dependent form of Nor (qNor), while the remaining MAGs (n = 8) encoded
438 the cytochrome c-dependent Nor (cNor) **(Suppl. Fig. S5c)**. In regards to the *nosZ* gene, most
439 MAGs (n = 6) contained sequences affiliated with the clade II (also known as atypical) NosZ [14,

440 15, 18] **(Suppl. Fig. S5d)**. Only four MAGs contained both the *norB* and *nosZ* genes and thus
441 have the potential to reduce NO completely to N_2 **(Fig. 3a)**.

442 As observed for the denitrifier *stricto sensu* communities, the communities of potential NO and
443 N_2O reducers also differed between the ecosystems **(Fig. 3b)**. MAGs assigned to the
444 Alphaproteobacteria class of the Proteobacteria were the most abundant in the barren,
445 heathland, and meadow soils. In particular, the MAG KWL-0112 assigned to the genera
446 *Reyranella* was the dominant *norB*-containing MAG, while KUL-0116 (belonging to an
447 uncharacterized genus in the family Acetobacteraceae) was the dominant MAG harbouring the
448 *nosZ* gene **(Suppl. Fig. S6**). On the other hand, fen communities were dominated by
449 Acidobacteriota MAGs **(Fig. 3b)**, particularly the *norB*- and *nosZ*-containing MAG KWL-0326
450 affiliated with the class Thermoanaerobaculia **(Suppl. Fig. S6)**. This MAG contained the same
451 set of genes encoding aerobic terminal oxidases as found in the *nirK*-containing Ellin6529 MAGs
452 that were dominant in the fen sites, namely *coxABC* and *cydAB* **(Suppl. Table S3)**. No genes
453 involved in carbon fixation, dissimilatory sulfate reduction, dissimilatory nitrate reduction to
454 ammonia, and nitrogen fixation were found in any of the dominant *norB*- and *nosZ*-containing
455 MAGs.

456 To elucidate the phylogenetic placement of the Acidobacteriota MAGs and to verify if the
457 potential for NO and N_2O reduction is present in other members of this phylum, we included in
458 our analysis all available genomes of Acidobacteriota strains and candidate taxa available on
459 GenBank. This revealed that genes encoding the Nir and Nos enzymes are widespread across
460 the phylum Acidobacteriota **(Fig. 4)**. Genes encoding the Nor enzyme were present in all but
461 one of the six Acidobacteriota subdivisions with genomes from cultured representatives. This
462 included the strains *Acidobacterium ailaaui* PMMR2 (subdivision Gp1), *Acidipila* sp. 4G-K13
463 (Gp1), *Silvibacterium bohemicum* DSM 103733 and *S. bohemicum* S15 (Gp1), Acidobacteriaceae
464 bacterium URHE0068 (Gp1), *Edaphobacter aggregans* DSM 19364 (Gp1), *Luteitalea pratensis*
465 DSM 100886 (Gp6), *Geothrix fermentans* DSM 14018 (Gp8), and *Thermoanaerobaculum*
466 *aquaticum* MP-01 (Gp23), as well as the candidate taxa *Candidatus* Koribacter versatilis
467 Ellin345 (Gp1), *Candidatus* Sulfotelmatomonas gaucii SbA5 (Gp1), and *Candidatus* Solibacter
468 usitatus Ellin6076 (Gp3). On the other hand, genes encoding the Nos enzyme were found only
469 in members of the subdivisions Gp6 and Gp23.

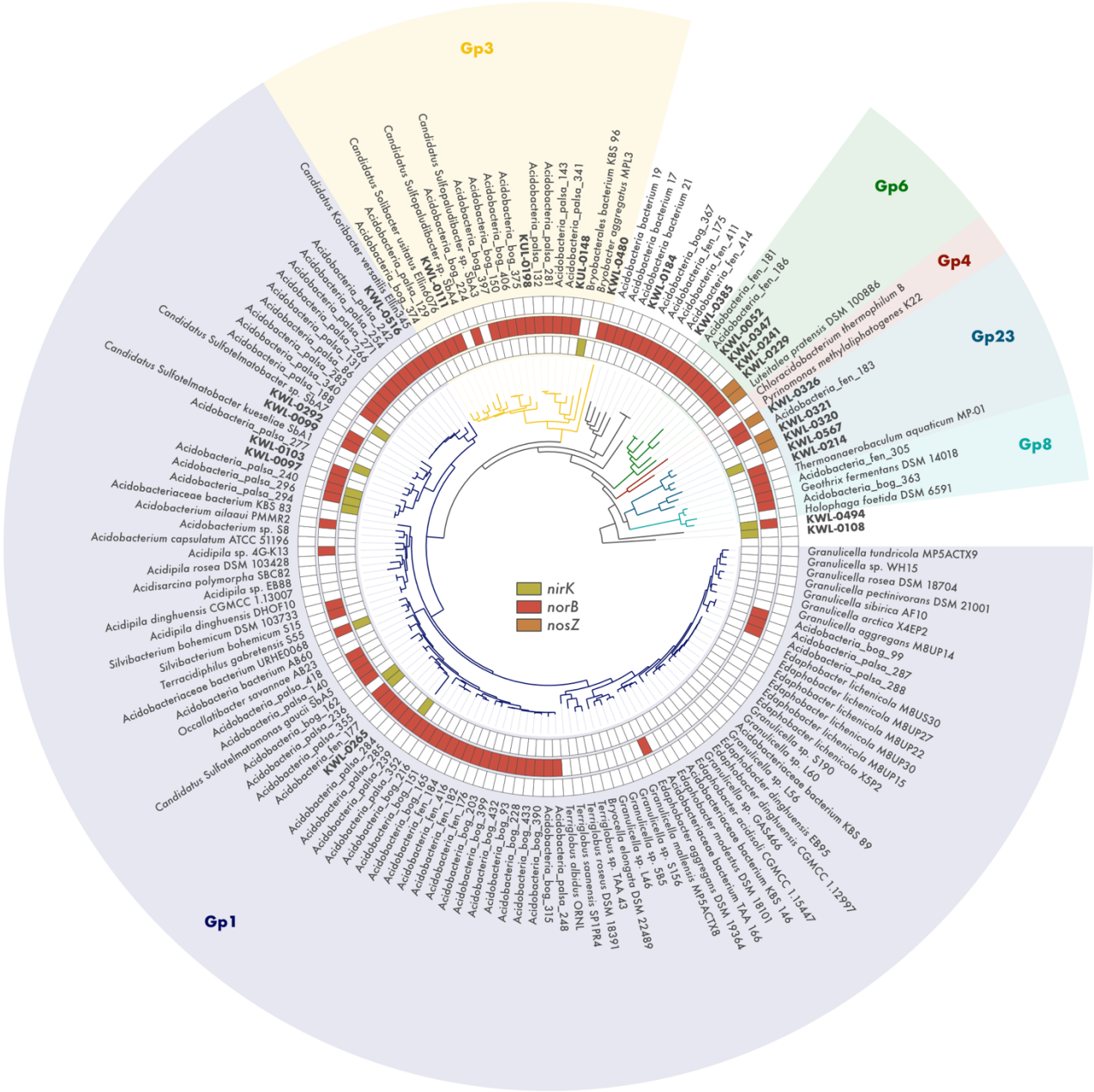

Fig. 4 | Metabolic potential for denitrification among members of the phylum Acidobacteriota. Phylogenomic analysis of 85 Acidobacteriota metagenome-assembled genomes (MAGs) containing denitrification genes recovered from tundra soils in Kilpisjärvi (northern Finland) and Stordalen Mire (northern Sweden), and 69 genomes of Acidobacteriota strains and candidate taxa. Maximum likelihood tree based on concatenated alignments of 23 ribosomal proteins and rooted with *Escherichia coli* ATCC 11775 (not shown). Genes encoding the nitrite (*nirK*), nitric oxide (*norB*), and nitrous oxide (*nosZ*) reductases were annotated using a three-step approach to avoid false positives (see methods).

478 # Discussion

479 The 796 MAGs obtained in the present study by a manual binning and curation effort represent
480 one of the largest genomic catalogues of microorganisms from tundra soils to date. Earlier gene-
481 centric investigations have revealed the potential for complete denitrification in tundra soils
482 [29, 87], however, these approaches fail to reveal the wider genomic context of the genes involved
483 in this pathway. By applying the genome-resolved metagenomics approach, we traced
484 denitrification genes to specific microbial populations, thereby allowing a detailed investigation
485 of the genomic makeup of potential denitrifiers in tundra soils. This approach also enabled us
486 to access the genomes of uncultured, poorly characterized taxa, which comprise the majority of
487 the microorganisms in soils and other complex ecosystems [33, 34]. Our genome-resolved survey
488 revealed that denitrification across different tundra soil ecosystems is dominated by
489 microorganisms with truncated denitrification pathways (i.e. harbouring only a subset of the
490 genes required for complete denitrification), most of which represent poorly characterized taxa
491 without cultured representatives. With the support of *in situ* measurements of N_2O fluxes, we
492 hypothesize that microorganisms with truncated denitrification pathways are important
493 drivers of N_2O cycling in tundra soils.

494 The congruence of these findings in both our original dataset of northern Finland soils and a re-
495 analysis of a comprehensive metagenomic dataset from soils in northern Sweden [37] suggests
496 that truncated denitrification pathways are not a methodological artifact arising from the
497 metabolic reconstruction of fragmented genomes. Indeed, recent genome-resolved investigations
498 have shown that cross-feeding between microorganisms with truncated metabolic pathways,
499 also known as metabolic handoffs, are the norm across a wide range of ecosystems such as
500 grassland soil, aquifer sediment, groundwater, and the ocean, and not only in relation to
501 denitrification but other redox transformations as well [21, 88, 89]. Although it is quite
502 established that denitrification is a community effort performed by different microbial
503 populations [12–15], genome-resolved metagenomic studies are beginning to reveal a more in-
504 depth, ecosystem-centric representation of the denitrification pathway. In addition to their
505 predominance in genomic databases [14], it appears that truncated denitrifiers are also
506 dominant within defined ecosystems across various terrestrial and aquatic biomes, including
507 the tundra. It has been suggested that the partitioning of metabolic pathways across different
508 populations via metabolic handoffs is advantageous as it eliminates competition between
509 enzymes accelerating substrate consumption [15, 22] and provides flexibility and resilience to
510 the communities in face of environmental disturbances [21]. We further hypothesize that the
511 predominance of denitrification pathways characterized mostly by metabolic handoffs in tundra

512 soils could be related to N limitation. If metabolic handoffs enable a more effective substrate
513 consumption as previously suggested [15, 22], truncated denitrification pathways would be
514 favoured in tundra soils which are mostly N limited but undergo rapid surges in N availability
515 e.g. during the spring melting season [90].

516 Our results showed that denitrifier communities in the tundra differ between drier upland
517 ecosystems (barren, heathland, and meadow soils) and water-logged fens. This is likely related
518 to differences in soil moisture affecting oxygen availability in these ecosystems. The dominant
519 denitrifier populations in the oxic dry upland soils, related to the genera *Bradyrhizobium*,
520 *Reyranella*, and other uncharacterized genera in the class Alphaproteobacteria, encoded aerobic
521 terminal oxidases that are active under highly aerobic conditions as well as oxidases with high
522 oxygen affinity [85, 86]. The former likely provides an adaptive advantage in these soils by
523 allowing rapid aerobic growth under standard conditions of high oxygen availability, and the
524 latter would sustain growth in microoxic niches within the soil matrix and during periods of
525 reduced oxygen availability (e.g. during the spring melting season).

526 On the other hand, fen soils are continuously inundated because the water table is at or near
527 the soil surface. The result is a mostly anoxic environment due to the slow rate at which oxygen
528 diffuses into the water-logged soil, favouring reduced rather than oxidized soil chemistry. In
529 line with this, we found a predominance of anaerobic processes in the fens, including a higher
530 abundance of genes involved in denitrification, sulfate reduction, and methanogenesis, the
531 latter supported by *in situ* measurements showing net CH_4 emission at the fen sites.
532 Communities of potential denitrifiers in the fen soils were dominated by somewhat enigmatic
533 taxa, namely potential NO_2^- reducers affiliated with the class Ellin6529 of the Chloroflexota
534 and NO/N_2O reducers assigned to the subdivision Gp23 of the Acidobacteriota. Both groups are
535 major members of microbial communities in soils worldwide [91], and RNA-based investigations
536 have shown that they are active in tundra soils during both summer and winter seasons [41,
537 92]. *Thermoanaerobaculum aquaticum* MP-01, the only cultivated member of the
538 Acidobacteriota subdivision Gp23, is a strictly anaerobic bacterium that has been shown to use
539 Fe and Mn, but not NO_3^- nor NO_2^-, as electron acceptors in anaerobic respiration [93]. However,
540 studies investigating the use of nitrogen oxides in anaerobic respiration usually provide soluble
541 NO_3^- or NO_2^- as electron acceptors, not the gases NO and N_2O, which bias against truncated
542 denitrifiers that do not contain the *narG* and *nirK*/*nirS* genes [94]. Ellin6529 – formerly G04 –
543 were first detected by culture-independent methods in alpine tundra wet meadow soil in the
544 Colorado Rocky Mountains, USA [95], and later isolated in a study targeting slow-growing and
545 mini-colony forming bacteria from Australian agricultural soil [96]. However, their ecological,
546 physiological, and metabolic preferences remain largely unknown. Their genomic composition

547 and high abundance in the water-logged, anoxic fen soils suggest that the Ellin6529 and Gp23
548 populations found in this study are likely able to grow anaerobically with the use of NO and
549 N_2O as electron acceptors. However, it is known that in addition to their role in anaerobic
550 respiration, NO and N_2O reduction can be used as a detoxification mechanism or as electron
551 sink for metabolism. For example, the aerobe *Gemmatimonas aurantica* T-27 is not able to grow
552 on N_2O alone, but can use N_2O as electron acceptor transiently when oxygen is depleted [97].

553 In addition to microbial community structure, differences in N_2O fluxes observed between
554 upland and fen soils also appear to be linked to soil moisture. Some of the drier upland sites
555 investigated were hotspots of N_2O consumption. This is particularly interesting for the acidic
556 heathland soils, as low pH is known to impair the expression of the NosZ enzyme thus promoting
557 N_2O emission [98, 99]. On the other hand, fens had close to net-zero N_2O fluxes, which is in line
558 with previous observations for water-saturated soils both in the tundra[7] and worldwide [11,
559 13]. This has been linked to lower rates of N mineralization and nitrification in anoxic
560 ecosystems, which limit the availability of NO_3^- and NO_2^- and promote complete denitrification,
561 resulting in N_2 as end product rather than N_2O. Indeed, supplementing fen soils in the tundra
562 with NO_3^- and NO_2^- has shown to promote N_2O emissions [100]. Moreover, climate change
563 models predict lowering of the water table in high-latitude wetlands, which could lead to
564 increased N_2O emissions from these ecosystems [101, 102].

565 Conclusions

566 A better understanding of denitrification is paramount for our ability to model N_2O emissions
567 and mitigate climate change. High-latitude environments in particular have experienced
568 amplified warming in recent decades, a trend that is likely to continue in the coming centuries.
569 As mechanisms of GHG emissions are very climate sensitive, the contribution of tundra soils to
570 global GHG atmospheric levels is thus predicted to increase in the future leading to a positive
571 feedback loop. Compared with carbon dioxide and CH_4, measurements of N_2O fluxes in tundra
572 soils are sparse and are rarely coupled with a characterization of the microorganisms involved,
573 making the magnitude and drivers of N_2O fluxes across the polar regions uncertain. While
574 microorganisms with truncated denitrification pathways appear to dominate the denitrifier
575 communities investigated here, the potential for complete denitrification was present at the
576 ecosystem level. In addition to a better monitoring of N_2O emissions throughout the tundra
577 biome, our results suggest that a better understanding of the contribution of tundra soil to global
578 N_2O levels relies on the elucidation of the regulatory mechanisms of metabolic handoffs in
579 communities dominated by truncated denitrifiers.

Declarations

Ethics approval and consent to participate

Not applicable.

Consent for publication

Not applicable.

Availability of data and materials

Raw metagenomic data and assembled MAGs have been submitted to the European Nucleotide Archive (ENA) under the project PRJEB41762. All the code used can be found in https://github.com/ArcticMicrobialEcology/Kilpisjarvi-MAGs.

Competing interests

The authors declare that they have no competing interests.

Funding

This work was funded by the Academy of Finland (grants 314114 and 335354) and the University of Helsinki. SV was funded by the Microbiology and Biotechnology Doctoral Programme (MBDP). AMV was funded by the Academy of Finland (grant 286950), the Otto Malm Foundation, and the Gordon and Betty Moore Foundation (grant 8414). MEM was supported by the Academy of Finland (grants 314630 and 317054).

Author contributions

JH and ML designed the research; SV and JH performed nucleic acid extraction and metagenomic library preparation; AMV and MEM designed and performed the GHG flux measurements and analyses; ISP analysed the data and wrote the manuscript; EER and TOD contributed with the analyses; all authors contributed to the final version of the manuscript.

Acknowledgements

We would like to acknowledge CSC – IT Centre for Science for providing the necessary computing resources and Kimmo Mattila for IT support; the staff from the Kilpisjärvi Biological Station, Tanja Orpana, Aino Rutanen, Anniina Sarekoski, Johanna Kerttula, and the members of the BioGeoClimate Modelling Lab for assistance with fieldwork and soil characterization; Jillian Banfield and Christina Biasi for helpful discussion; Laura Cappelatti for proof-reading

the manuscript; Murat Eren, Sebastian Lücker, Donovan Parks, and Antonios Kioukis for tips, recommendations, and troubleshooting; and all anonymous reviewers who provided important insights to the original manuscript.

References

1. IPCC, editor. Climate Change 2013: The Physical Science Basis. Contribution of Working Group I to the Fifth Assessment Report of the Intergovernmental Panel on Climate Change. Cambridge: Cambridge University Press; 2013. doi:10.1017/CBO9781107415324.

2. Tian H, Xu R, Canadell JG, Thompson RL, Winiwarter W, Suntharalingam P, et al. A comprehensive quantification of global nitrous oxide sources and sinks. Nature. 2020;586:248–56.

3. Repo ME, Susiluoto S, Lind SE, Jokinen S, Elsakov V, Biasi C, et al. Large N2O emissions from cryoturbated peat soil in tundra. Nat Geosci. 2009;2:189–92.

4. Marushchak ME, Pitkämäki A, Koponen H, Biasi C, Seppälä M, Martikainen PJ. Hot spots for nitrous oxide emissions found in different types of permafrost peatlands. Glob Change Biol. 2011;17:2601–14.

5. Stewart KJ, Grogan P, Coxson DS, Siciliano SD. Topography as a key factor driving atmospheric nitrogen exchanges in arctic terrestrial ecosystems. Soil Biol Biochem. 2014;70:96–112.

6. Voigt C, Marushchak ME, Lamprecht RE, Jackowicz-Korczyński M, Lindgren A, Mastepanov M, et al. Increased nitrous oxide emissions from Arctic peatlands after permafrost thaw. Proc Natl Acad Sci. 2017;114:6238–43.

7. Voigt C, Marushchak ME, Abbott BW, Biasi C, Elberling B, Siciliano SD, et al. Nitrous oxide emissions from permafrost-affected soils. Nat Rev Earth Environ. 2020;1:420–34.

8. Schuur EAG, McGuire AD, Schädel C, Grosse G, Harden JW, Hayes DJ, et al. Climate change and the permafrost carbon feedback. Nature. 2015;520:171–9.

9. Hugelius G, Loisel J, Chadburn S, Jackson RB, Jones M, MacDonald G, et al. Large stocks of peatland carbon and nitrogen are vulnerable to permafrost thaw. Proc Natl Acad Sci. 2020;117:20438–46.

10. Post E, Alley RB, Christensen TR, Macias-Fauria M, Forbes BC, Gooseff MN, et al. The polar regions in a 2°C warmer world. Sci Adv. 2019;5:eaaw9883.

638 11. Butterbach-Bahl K, Baggs EM, Dannenmann M, Kiese R, Zechmeister-Boltenstern S.
639 Nitrous oxide emissions from soils: how well do we understand the processes and their controls?
640 Philos Trans R Soc B Biol Sci. 2013;368:20130122.

641 12. Zumft WG. Cell biology and molecular basis of denitrification. Microbiol Mol Biol Rev
642 MMBR. 1997;61:533–616.

643 13. Wallenstein MD, Myrold DD, Firestone M, Voytek M. Environmental controls on
644 denitrifying communities and denitrification rates: insights from molecular methods. Ecol Appl.
645 2006;16:2143–52.

646 14. Graf DRH, Jones CM, Hallin S. Intergenomic Comparisons Highlight Modularity of the
647 Denitrification Pathway and Underpin the Importance of Community Structure for N2O
648 Emissions. PLoS ONE. 2014;9:e114118.

649 15. Hallin S, Philippot L, Löffler FE, Sanford RA, Jones CM. Genomics and Ecology of Novel
650 N2O-Reducing Microorganisms. Trends Microbiol. 2018;26:43–55.

651 16. Bakken LR, Bergaust L, Liu B, Frostegård Å. Regulation of denitrification at the cellular
652 level: a clue to the understanding of N_2O emissions from soils. Philos Trans R Soc B Biol Sci.
653 2012;367:1226–34.

654 17. Philippot L, Andert J, Jones CM, Bru D, Hallin S. Importance of denitrifiers lacking the
655 genes encoding the nitrous oxide reductase for N2O emissions from soil: role of denitrifier
656 diversity for N2O fluxes. Glob Change Biol. 2011;17:1497–504.

657 18. Sanford RA, Wagner DD, Wu Q, Chee-Sanford JC, Thomas SH, Cruz-Garcia C, et al.
658 Unexpected nondenitrifier nitrous oxide reductase gene diversity and abundance in soils. Proc
659 Natl Acad Sci. 2012;109:19709–14.

660 19. Jones CM, Graf DR, Bru D, Philippot L, Hallin S. The unaccounted yet abundant nitrous
661 oxide-reducing microbial community: a potential nitrous oxide sink. ISME J. 2013;7:417–26.

662 20. Jones CM, Spor A, Brennan FP, Breuil M-C, Bru D, Lemanceau P, et al. Recently identified
663 microbial guild mediates soil N2O sink capacity. Nat Clim Change. 2014;4:801–5.

664 21. Anantharaman K, Brown CT, Hug LA, Sharon I, Castelle CJ, Probst AJ, et al. Thousands
665 of microbial genomes shed light on interconnected biogeochemical processes in an aquifer
666 system. Nat Commun. 2016;7:13219.

667 22. Lilja EE, Johnson DR. Segregating metabolic processes into different microbial cells
668 accelerates the consumption of inhibitory substrates. ISME J. 2016;10:1568–78.

669 23. Liu X-Y, Koba K, Koyama LA, Hobbie SE, Weiss MS, Inagaki Y, et al. Nitrate is an important
670 nitrogen source for Arctic tundra plants. Proc Natl Acad Sci. 2018;115:3398–403.

671 24. Kou D, Yang G, Li F, Feng X, Zhang D, Mao C, et al. Progressive nitrogen limitation across
672 the Tibetan alpine permafrost region. Nat Commun. 2020;11:3331.

673 25. Yergeau E, Kang S, He Z, Zhou J, Kowalchuk GA. Functional microarray analysis of
674 nitrogen and carbon cycling genes across an Antarctic latitudinal transect. ISME J. 2007;1:163–
675 79.

676 26. Yergeau E, Hogues H, Whyte LG, Greer CW. The functional potential of high Arctic
677 permafrost revealed by metagenomic sequencing, qPCR and microarray analyses. ISME J.
678 2010;4:1206–14.

679 27. Palmer K, Biasi C, Horn MA. Contrasting denitrifier communities relate to contrasting N2O
680 emission patterns from acidic peat soils in arctic tundra. ISME J. 2012;6:1058–77.

681 28. Dai H-T, Zhu R-B, Sun B-W, Che C-S, Hou L-J. Effects of Sea Animal Activities on Tundra
682 Soil Denitrification and nirS- and nirK-Encoding Denitrifier Community in Maritime
683 Antarctica. Front Microbiol. 2020;11:573302.

684 29. Ortiz M, Bosch J, Coclet C, Johnson J, Lebre P, Salawu-Rotimi A, et al. Microbial Nitrogen
685 Cycling in Antarctic Soils. Microorganisms. 2020;8:1442.

686 30. Brummell ME, Farrell RE, Siciliano SD. Greenhouse gas soil production and surface fluxes
687 at a high arctic polar oasis. Soil Biol Biochem. 2012;52:1–12.

688 31. Chapuis-Lardy L, Wrage N, Metay A, Chotte J-L, Bernoux M. Soils, a sink for N_2O? A
689 review. Glob Change Biol. 2007;13:1–17.

690 32. Yu T, Zhuang Q. Quantifying global N2O emissions from natural ecosystem soils using trait-
691 based biogeochemistry models. Biogeosciences. 2019;16:207–22.

692 33. Rappé MS, Giovannoni SJ. The Uncultured Microbial Majority. Annu Rev Microbiol.
693 2003;57:369–94.

694 34. Steen AD, Crits-Christoph A, Carini P, DeAngelis KM, Fierer N, Lloyd KG, et al. High
695 proportions of bacteria and archaea across most biomes remain uncultured. ISME J.
696 2019;13:3126–30.

697 35. Mackelprang R, Waldrop MP, DeAngelis KM, David MM, Chavarria KL, Blazewicz SJ, et
698 al. Metagenomic analysis of a permafrost microbial community reveals a rapid response to thaw.
699 Nature. 2011;480:368–71.

700 36. Hultman J, Waldrop MP, Mackelprang R, David MM, McFarland J, Blazewicz SJ, et al.
701 Multi-omics of permafrost, active layer and thermokarst bog soil microbiomes. Nature.
702 2015;521:208–12.

703 37. Woodcroft BJ, Singleton CM, Boyd JA, Evans PN, Emerson JB, Zayed AAF, et al. Genome-
704 centric view of carbon processing in thawing permafrost. Nature. 2018;560:49–54.

705 38. Pirinen P, Simola H, Aalto J, Kaukoranta J-P, Karlsson P, Ruuhela R. Climatological
706 statistics of Finland 1981–2010. Helsinki: Finnish Meteorological Institute; 2012.

707 39. le Roux PC, Aalto J, Luoto M. Soil moisture's underestimated role in climate change impact
708 modelling in low-energy systems. Glob Change Biol. 2013;19:2965–75.

709 40. Niittynen P, Heikkinen RK, Aalto J, Guisan A, Kemppinen J, Luoto M. Fine-scale tundra
710 vegetation patterns are strongly related to winter thermal conditions. Nat Clim Change. 2020.
711 doi:10.1038/s41558-020-00916-4.

712 41. Viitamäki S, Pessi IS, Virkkala A-M, Niittynen P, Kemppinen J, Eronen-Rasimus E, et al.
713 The activity and functions of subarctic soil microbial communities vary across vegetation types.
714 bioRxiv. 2021. doi:10.1101/2021.06.12.448001.

715 42. le Roux PC, Pellissier L, Wisz MS, Luoto M. Incorporating dominant species as proxies for
716 biotic interactions strengthens plant community models. J Ecol. 2014;102:767–75.

717 43. Kemppinen J, Niittynen P, Aalto J, le Roux PC, Luoto M. Water as a resource, stress and
718 disturbance shaping tundra vegetation. Oikos. 2019;128:811–22.

719 44. Livingston GP, Hutchinson GL. Enclosure-based measurement of trace gas exchange:
720 applications and sources of error. In: Biogenic trace gases: Measuring emissions from soil and
721 water. Oxford, United Kingdom: Blackwell Science. p. 14–51.

722 45. R Core Team. R: A language and environment for statistical computing. 2020.

723 46. Andrews S. FastQC: A Quality Control Tool for High Throughput Sequence Data. 2019.
724 http://www.bioinformatics.babraham.ac.uk/projects/fastqc/.

725 47. Ewels P, Magnusson M, Lundin S, Käller M. MultiQC: summarize analysis results for
726 multiple tools and samples in a single report. Bioinformatics. 2016;32:3047–8.

727 48. Martin M. Cutadapt removes adapter sequences from high-throughput sequencing reads.
728 EMBnet.journal. 2011;17:10.

729 49. Leger A, Leonardi T. pycoQC, interactive quality control for Oxford Nanopore Sequencing.
730 J Open Source Softw. 2019;4:1236.

731 50. Wick RR. Porechop. 2018. https://github.com/rrwick/Porechop.

732 51. Li H. seqtk. 2018. https://github.com/lh3/seqtk.

733 52. Bengtsson-Palme J, Hartmann M, Eriksson KM, Pal C, Thorell K, Larsson DGJ, et al.
734 METAXA 2: improved identification and taxonomic classification of small and large subunit
735 rRNA in metagenomic data. Mol Ecol Resour. 2015;15:1403–14.

736 53. Quast C, Pruesse E, Yilmaz P, Gerken J, Schweer T, Yarza P, et al. The SILVA ribosomal
737 RNA gene database project: improved data processing and web-based tools. Nucleic Acids Res.
738 2012;41:D590–6.

739 54. Schloss PD, Westcott SL, Ryabin T, Hall JR, Hartmann M, Hollister EB, et al. Introducing
740 mothur: Open-Source, Platform-Independent, Community-Supported Software for Describing
741 and Comparing Microbial Communities. Appl Environ Microbiol. 2009;75:7537–41.

742 55. Wang Q, Garrity GM, Tiedje JM, Cole JR. Naïve Bayesian Classifier for Rapid Assignment
743 of rRNA Sequences into the New Bacterial Taxonomy. Appl Environ Microbiol. 2007;73:5261–
744 7.

745 56. Oksanen J, Blanchet FG, Friendly M, Kindt R, Legendre P, McGlinn D, et al. vegan:
746 Community Ecology Package. 2019. https://CRAN.R-project.org/package=vegan.

747 57. Li D, Liu C-M, Luo R, Sadakane K, Lam T-W. MEGAHIT: an ultra-fast single-node solution
748 for large and complex metagenomics assembly via succinct de Bruijn graph. Bioinformatics.
749 2015;31:1674–6.

750 58. Kolmogorov M, Bickhart DM, Behsaz B, Gurevich A, Rayko M, Shin SB, et al. metaFlye:
751 scalable long-read metagenome assembly using repeat graphs. Nat Methods. 2020.
752 doi:10.1038/s41592-020-00971-x.

753 59. Langmead B, Salzberg SL. Fast gapped-read alignment with Bowtie 2. Nat Methods.
754 2012;9:357–9.

755 60. Li H, Handsaker B, Wysoker A, Fennell T, Ruan J, Homer N, et al. The Sequence
756 Alignment/Map format and SAMtools. Bioinformatics. 2009;25:2078–9.

757 61. Walker BJ, Abeel T, Shea T, Priest M, Abouelliel A, Sakthikumar S, et al. Pilon: An
758 Integrated Tool for Comprehensive Microbial Variant Detection and Genome Assembly
759 Improvement. PLoS ONE. 2014;9:e112963.

760 62. Mikheenko A, Saveliev V, Gurevich A. MetaQUAST: evaluation of metagenome assemblies.
761 Bioinformatics. 2016;32:1088–90.

762 63. Eren AM, Esen ÖC, Quince C, Vineis JH, Morrison HG, Sogin ML, et al. Anvi'o: an advanced
763 analysis and visualization platform for 'omics data. PeerJ. 2015;3:e1319.

764 64. Hyatt D, Chen G-L, LoCascio PF, Land ML, Larimer FW, Hauser LJ. Prodigal: prokaryotic
765 gene recognition and translation initiation site identification. BMC Bioinformatics.
766 2010;11:119.

767 65. Eddy SR. Accelerated Profile HMM Searches. PLoS Comput Biol. 2011;7:e1002195.

768 66. Buchfink B, Xie C, Huson DH. Fast and sensitive protein alignment using DIAMOND. Nat
769 Methods. 2015;12:59–60.

770 67. Parks DH, Chuvochina M, Waite DW, Rinke C, Skarshewski A, Chaumeil P-A, et al. A
771 standardized bacterial taxonomy based on genome phylogeny substantially revises the tree of
772 life. Nat Biotechnol. 2018;36:996–1004.

773 68. Parks DH, Chuvochina M, Chaumeil P-A, Rinke C, Mussig AJ, Hugenholtz P. A complete
774 domain-to-species taxonomy for Bacteria and Archaea. Nat Biotechnol. 2020.
775 doi:10.1038/s41587-020-0501-8.

776 69. Alneberg J, Bjarnason BS, de Bruijn I, Schirmer M, Quick J, Ijaz UZ, et al. Binning
777 metagenomic contigs by coverage and composition. Nat Methods. 2014;11:1144–6.

778 70. Aramaki T, Blanc-Mathieu R, Endo H, Ohkubo K, Kanehisa M, Goto S, et al. KofamKOALA:
779 KEGG Ortholog assignment based on profile HMM and adaptive score threshold.
780 Bioinformatics. 2020;36:2251–2.

781 71. Katoh K, Standley DM. MAFFT Multiple Sequence Alignment Software Version 7:
782 Improvements in Performance and Usability. Mol Biol Evol. 2013;30:772–80.

783 72. Okonechnikov K, Golosova O, Fursov M. Unipro UGENE: a unified bioinformatics toolkit.
784 Bioinformatics. 2012;28:1166–7.

785 73. Decleyre H, Heylen K, Tytgat B, Willems A. Highly diverse nirK genes comprise two major
786 clades that harbour ammonium-producing denitrifiers. BMC Genomics. 2016;17:155.

787 74. Li Y, Bali S, Borg S, Katzmann E, Ferguson SJ, Schuler D. Cytochrome cd1 Nitrite
788 Reductase NirS Is Involved in Anaerobic Magnetite Biomineralization in Magnetospirillum
789 gryphiswaldense and Requires NirN for Proper d1 Heme Assembly. J Bacteriol. 2013;195:4297–
790 309.

791 75. Heylen K, Keltjens J. Redundancy and modularity in membrane-associated dissimilatory
792 nitrate reduction in Bacillus. Front Microbiol. 2012;3. doi:10.3389/fmicb.2012.00371.

793 76. Price MN, Dehal PS, Arkin AP. FastTree 2 – Approximately Maximum-Likelihood Trees for
794 Large Alignments. PLoS ONE. 2010;5:e9490.

795 77. Woodcroft BJ. CoverM. 2021.

796 78. Li H. Minimap and miniasm: fast mapping and de novo assembly for noisy long sequences.
797 Bioinformatics. 2016;32:2103–10.

798 79. Chaumeil P-A, Mussig AJ, Hugenholtz P, Parks DH. GTDB-Tk: a toolkit to classify genomes
799 with the Genome Taxonomy Database. Bioinformatics. 2019;:btz848.

800 80. Edgar RC. MUSCLE: multiple sequence alignment with high accuracy and high throughput.
801 Nucleic Acids Res. 2004;32:1792–7.

802 81. Zhang H, Yohe T, Huang L, Entwistle S, Wu P, Yang Z, et al. dbCAN2: a meta server for
803 automated carbohydrate-active enzyme annotation. Nucleic Acids Res. 2018;46:W95–101.

804 82. Jain C, Rodriguez-R LM, Phillippy AM, Konstantinidis KT, Aluru S. High throughput ANI
805 analysis of 90K prokaryotic genomes reveals clear species boundaries. Nat Commun.
806 2018;9:5114.

807 83. Borisov VB, Gennis RB, Hemp J, Verkhovsky MI. The cytochrome bd respiratory oxygen
808 reductases. Biochim Biophys Acta BBA - Bioenerg. 2011;1807:1398–413.

809 84. Giuffrè A, Borisov VB, Arese M, Sarti P, Forte E. Cytochrome bd oxidase and bacterial
810 tolerance to oxidative and nitrosative stress. Biochim Biophys Acta BBA - Bioenerg.
811 2014;1837:1178–87.

812 85. Dinamarca MA, Ruiz-Manzano A, Rojo F. Inactivation of Cytochrome *o* Ubiquinol Oxidase
813 Relieves Catabolic Repression of the *Pseudomonas putida* GPo1 Alkane Degradation Pathway.
814 J Bacteriol. 2002;184:3785–93.

815 86. Bueno E, Mesa S, Bedmar EJ, Richardson DJ, Delgado MJ. Bacterial Adaptation of
816 Respiration from Oxic to Microoxic and Anoxic Conditions: Redox Control. Antioxid Redox
817 Signal. 2012;16:819–52.

818 87. Makhalanyane TP, Van Goethem MW, Cowan DA. Microbial diversity and functional
819 capacity in polar soils. Curr Opin Biotechnol. 2016;38:159–66.

820 88. Diamond S, Andeer PF, Li Z, Crits-Christoph A, Burstein D, Anantharaman K, et al.
821 Mediterranean grassland soil C–N compound turnover is dependent on rainfall and depth, and
822 is mediated by genomically divergent microorganisms. Nat Microbiol. 2019;4:1356–67.

823 89. Sun X, Ward BB. Novel metagenome-assembled genomes involved in the nitrogen cycle from
824 a Pacific oxygen minimum zone. ISME Commun. 2021;1:26.

825 90. Westergaard-Nielsen A, Balstrøm T, Treier UA, Normand S, Elberling B. Estimating
826 meltwater retention and associated nitrate redistribution during snowmelt in an Arctic tundra
827 landscape. Environ Res Lett. 2020;15:034025.

828 91. Delgado-Baquerizo M, Oliverio AM, Brewer TE, Benavent-González A, Eldridge DJ,
829 Bardgett RD, et al. A global atlas of the dominant bacteria found in soil. Science. 2018;359:320–
830 5.

831 92. Männistö MK, Kurhela E, Tiirola M, Häggblom MM. Acidobacteria dominate the active
832 bacterial communities of Arctic tundra with widely divergent winter-time snow accumulation
833 and soil temperatures. FEMS Microbiol Ecol. 2013;84:47–59.

834 93. Losey NA, Stevenson BS, Busse H-J, Damsté JSS, Rijpstra WIC, Rudd S, et al.
835 Thermoanaerobaculum aquaticum gen. nov., sp. nov., the first cultivated member of
836 Acidobacteria subdivision 23, isolated from a hot spring. Int J Syst Evol Microbiol. 2013;63
837 Pt_11:4149–57.

838 94. Lycus P, Lovise Bøthun K, Bergaust L, Peele Shapleigh J, Reier Bakken L, Frostegård Å.
839 Phenotypic and genotypic richness of denitrifiers revealed by a novel isolation strategy. ISME
840 J. 2017;11:2219–32.

841 95. Costello EK, Schmidt SK. Microbial diversity in alpine tundra wet meadow soil: novel
842 Chloroflexi from a cold, water-saturated environment. Environ Microbiol. 2006;8:1471–86.

843 96. Davis KER, Sangwan P, Janssen PH. Acidobacteria, Rubrobacteridae and Chloroflexi are
844 abundant among very slow-growing and mini-colony-forming soil bacteria. Environ Microbiol.
845 2011;13:798–805.

846 97. Park D, Kim H, Yoon S. Nitrous Oxide Reduction by an Obligate Aerobic Bacterium,
847 Gemmatimonas aurantiaca Strain T-27. Appl Environ Microbiol. 2017;83.
848 doi:10.1128/AEM.00502-17.

849 98. Liu B, Frostegård Å, Bakken LR. Impaired Reduction of N_2O to N_2 in Acid Soils Is Due to
850 a Posttranscriptional Interference with the Expression of *nosZ*. mBio. 2014;5.
851 doi:10.1128/mBio.01383-14.

852 99. Samad MS, Biswas A, Bakken LR, Clough TJ, de Klein CAM, Richards KG, et al.
853 Phylogenetic and functional potential links pH and N2O emissions in pasture soils. Sci Rep.
854 2016;6:35990.

855 100. Palmer K, Horn MA. Denitrification Activity of a Remarkably Diverse Fen Denitrifier
856 Community in Finnish Lapland Is N-Oxide Limited. PLOS ONE. 2015;10:e0123123.

857 101. Smith K. The potential for feedback effects induced by global warming on emissions of
858 nitrous oxide by soils. Glob Change Biol. 1997;3:327–38.

859 102. Kåresdotter E, Destouni G, Ghajarnia N, Hugelius G, Kalantari Z. Mapping the
860 Vulnerability of Arctic Wetlands to Global Warming. Earths Future. 2021;9.
861 doi:10.1029/2020EF001858.

Supplementary Figures

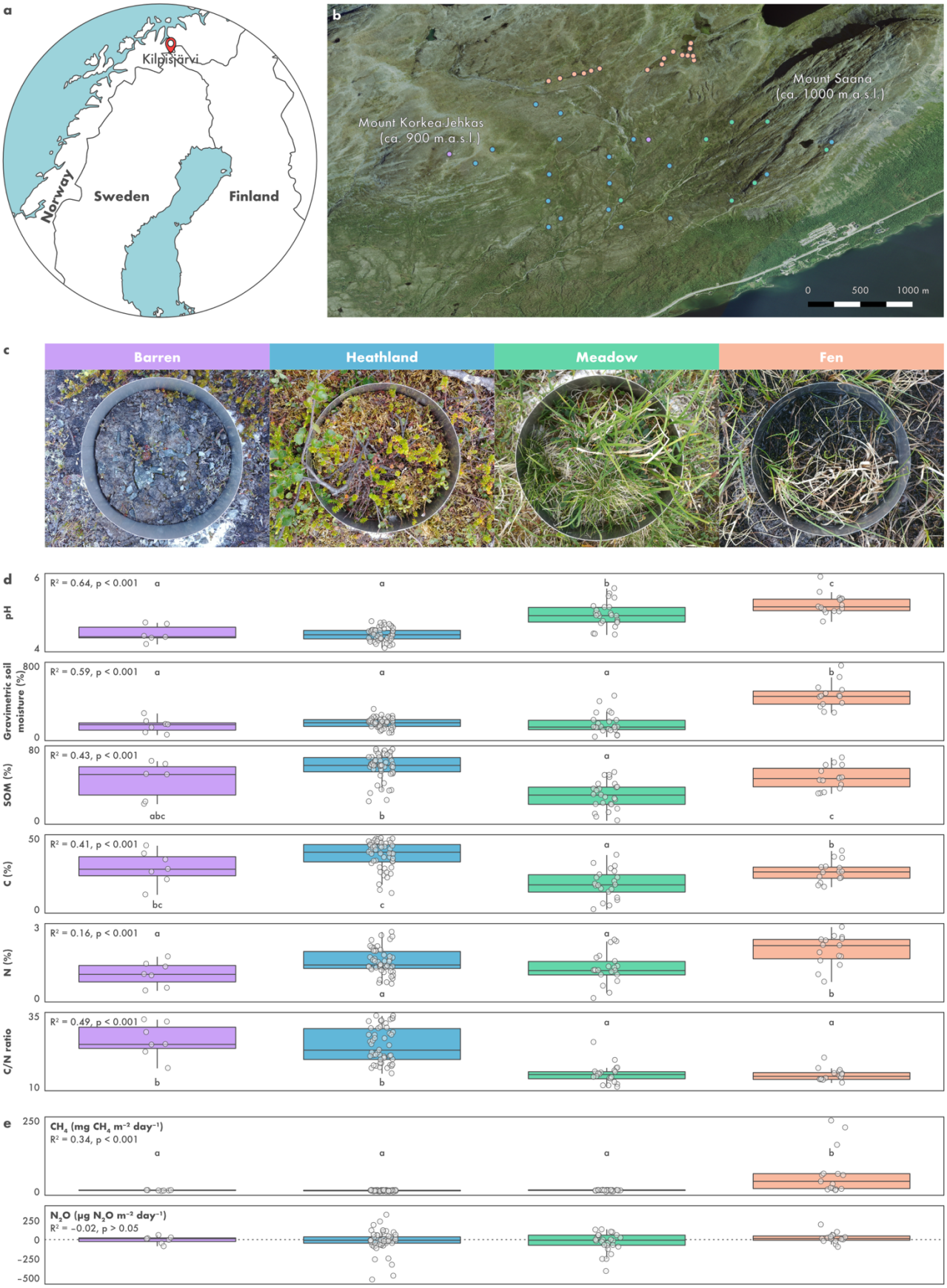

(Previous page) Suppl. Fig. S1 | Saana Nature Reserve, an area of mountain tundra in Kilpisjärvi, northern Finland. a) Map of Fennoscandia showing the location of Kilpisjärvi. **b)** Aerial overview of the study area showing the location of the 43 sites sampled for metagenomic analysis. Image provided by the National Land Survey of Finland under the Creative Commons CC BY 4.0 license. **c)** Pictures of the four types of soil ecosystems investigated. **d)** Physicochemical characterization of the soil ecosystems based on an extended set of 228 samples taken from the organic layer. **e)** *In situ* ecosystem-level nitrous oxide (N_2O) and methane (CH_4) fluxes measured from 101 sites using a static, non-steady state, non-flow-through system. Negative values represent net uptake and positive net emissions. For clarity, one outlier measurement from a meadow site (660 μg N_2O m^{-2} day^{-1}) was removed.

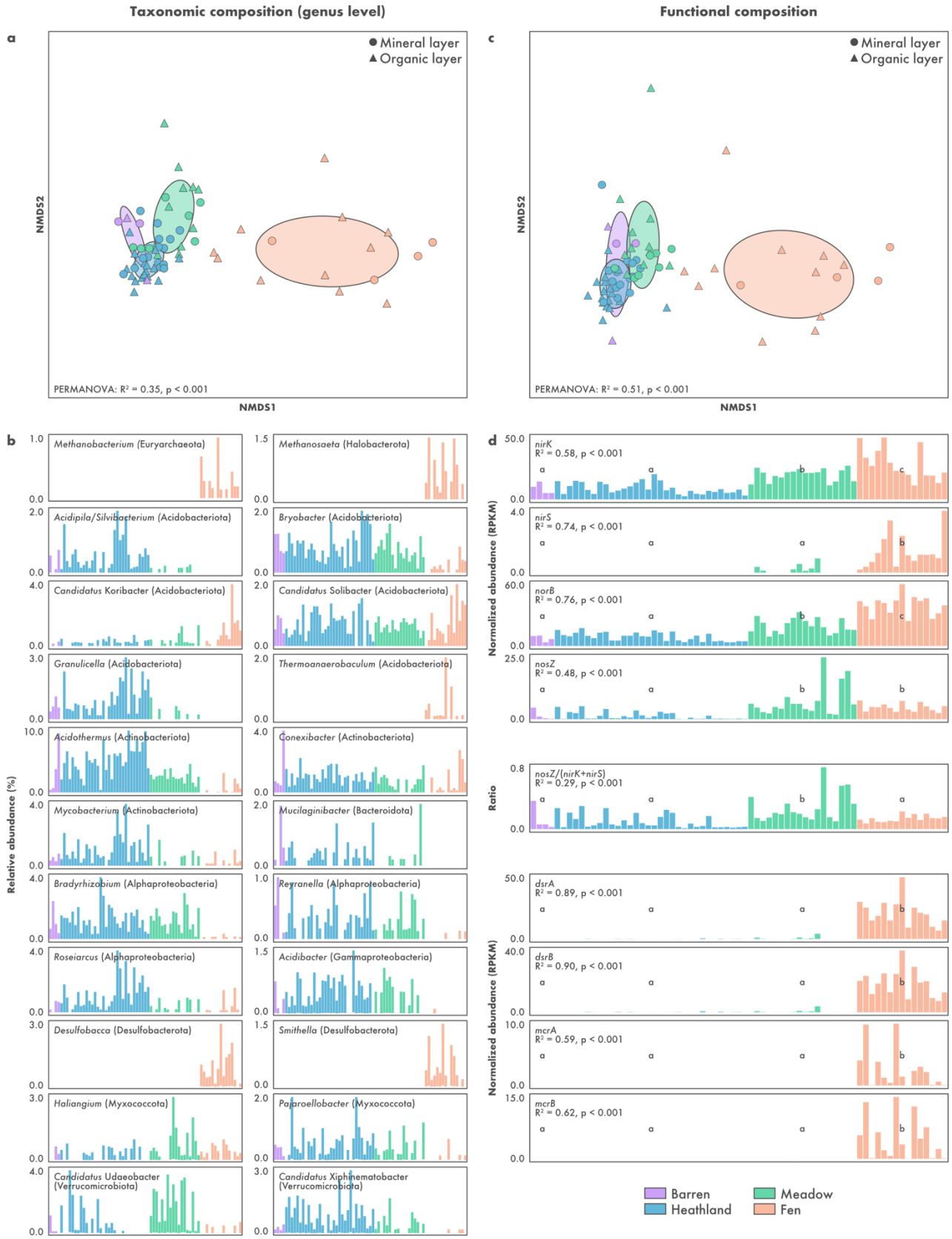
Taxonomic composition (genus level)
Functional composition
a
Mineral layer
Organic layer
NMDS2
NMDS1
PERMANOVA: R² = 0.35, p < 0.001
c
PERMANOVA: R² = 0.51, p < 0.001
b
Relative abundance (%)
Methanobacterium (Euryarchaeota)
Methanosaeta (Halobacterota)
Acidipila/Silvibacterium (Acidobacteriota)
Bryobacter (Acidobacteriota)
Candidatus Koribacter (Acidobacteriota)
Candidatus Solibacter (Acidobacteriota)
Granulicella (Acidobacteriota)
Thermoanaerobaculum (Acidobacteriota)
Acidothermus (Actinobacteriota)
Conexibacter (Actinobacteriota)
Mycobacterium (Actinobacteriota)
Mucilaginibacter (Bacteroidota)
Bradyrhizobium (Alphaproteobacteria)
Reyranella (Alphaproteobacteria)
Roseiarcus (Alphaproteobacteria)
Acidibacter (Gammaproteobacteria)
Desulfobacca (Desulfobacterota)
Smithella (Desulfobacterota)
Haliangium (Myxococcota)
Pajaroellobacter (Myxococcota)
Candidatus Udaeobacter (Verrucomicrobiota)
Candidatus Xiphinematobacter (Verrucomicrobiota)
d
Normalized abundance (RPKM)
Ratio
nirK
R² = 0.58, p < 0.001
nirS
R² = 0.74, p < 0.001
norB
R² = 0.76, p < 0.001
nosZ
R² = 0.48, p < 0.001
nosZ/(nirK+nirS)
R² = 0.29, p < 0.001
dsrA
R² = 0.89, p < 0.001
dsrB
R² = 0.90, p < 0.001
mcrA
R² = 0.59, p < 0.001
mcrB
R² = 0.62, p < 0.001
Barren
Meadow
Heathland
Fen

(Previous page) Suppl. Fig. S2 | The microbial diversity of Kilpisjärvi soils as seen using a read-based gene-centric approach. Taxonomic composition was computed based on the annotation of unassembled SSU rRNA gene sequences against the SILVA database. Functional annotation was done by searching assembled genes against the KOfam database. The annotation of putative denitrification genes was confirmed using a phylogenetic approach. **a, c)** Non-metric multidimensional scaling (NMDS) of taxonomic and functional community structure, respectively. Differences between the ecosystems were assessed using permutational ANOVA (PERMANOVA). **b)** Abundance profile of the five most abundant genera in each ecosystem. **d)** Abundance profile of marker genes for denitrification, sulfate reduction, and methanogenesis.

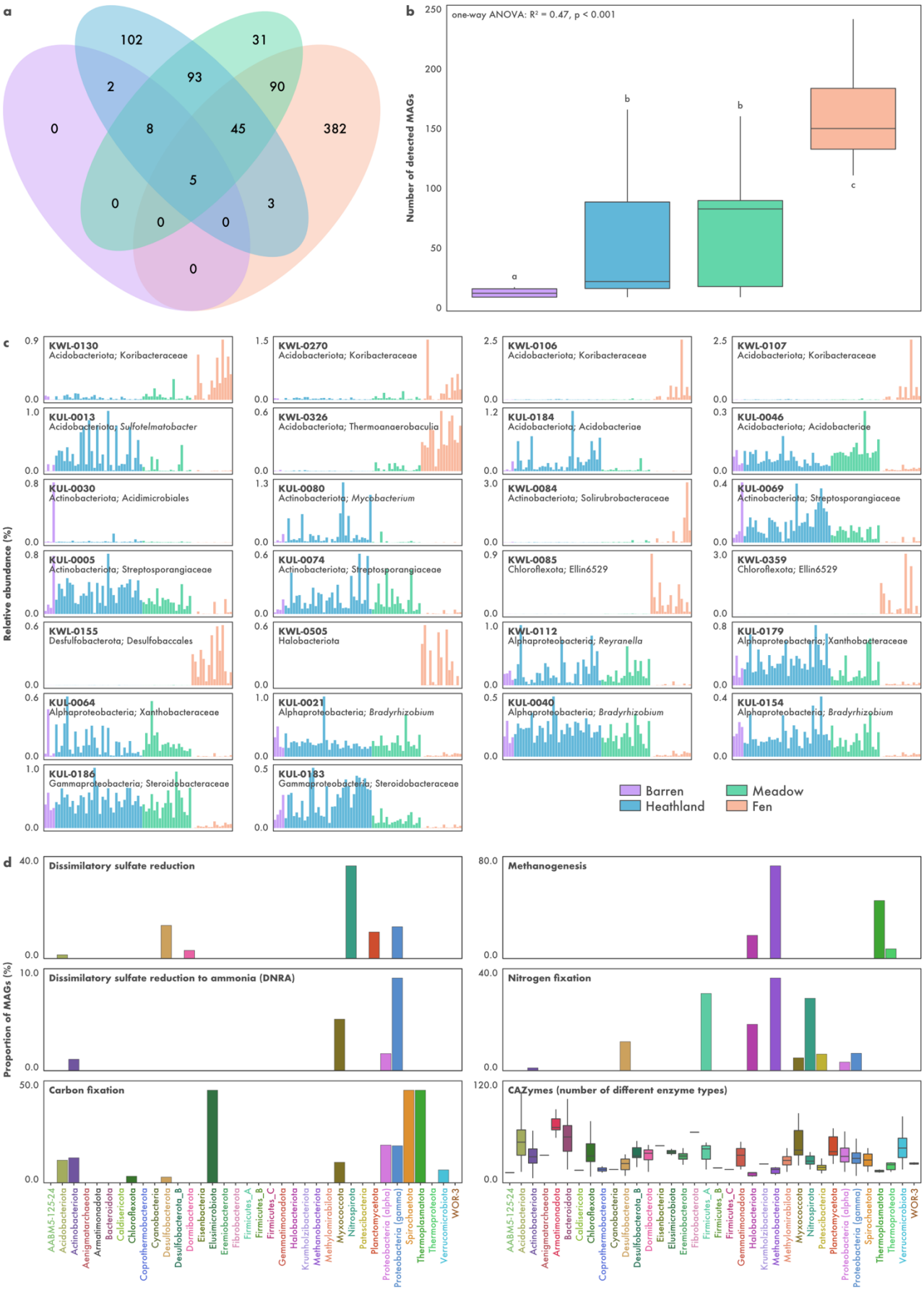
a
102
31
2
93
90
0
8
45
382
5
0
3
0
0
0
b
one-way ANOVA: R² = 0.47, p < 0.001
Number of detected MAGs
250
200
150
100
50
0
a
b
b
c
c
Relative abundance (%)
KWL-0130
Acidobacteriota; Koribacteraceae
KWL-0270
Acidobacteriota; Koribacteraceae
KWL-0106
Acidobacteriota; Koribacteraceae
KWL-0107
Acidobacteriota; Koribacteraceae
KUL-0013
Acidobacteriota; Sulfotelmatobacter
KUL-0326
Acidobacteriota; Thermoanaerobaculia
KUL-0184
Acidobacteriota; Acidobacteriae
KUL-0046
Acidobacteriota; Acidobacteriae
KUL-0030
Actinobacteriota; Acidimicrobiales
KUL-0080
Actinobacteriota; Mycobacterium
KWL-0084
Actinobacteriota; Solirubrobacteraceae
KUL-0069
Actinobacteriota; Streptosporangiaceae
KUL-0005
Actinobacteriota; Streptosporangiaceae
KUL-0074
Actinobacteriota; Streptosporangiaceae
KWL-0085
Chloroflexota; Ellin6529
KWL-0359
Chloroflexota; Ellin6529
KWL-0155
Desulfobacterota; Desulfobaccales
KWL-0505
Halobacteriota
KUL-0112
Alphaproteobacteria; Reyranella
KUL-0179
Alphaproteobacteria; Xanthobacteraceae
KUL-0064
Alphaproteobacteria; Xanthobacteraceae
KUL-0021
Alphaproteobacteria; Bradyrhizobium
KUL-0040
Alphaproteobacteria; Bradyrhizobium
KUL-0154
Alphaproteobacteria; Bradyrhizobium
KUL-0186
Gammaproteobacteria; Steroidobacteraceae
KUL-0183
Gammaproteobacteria; Steroidobacteraceae
Barren
Heathland
Meadow
Fen
d
Proportion of MAGs (%)
Dissimilatory sulfate reduction
Methanogenesis
Dissimilatory sulfate reduction to ammonia (DNRA)
Nitrogen fixation
Carbon fixation
CAZymes (number of different enzyme types)
AABM5-125-24
Acidobacteriota
Actinobacteriota
Aenigmatarchaeota
Armatimonadota
Bacteroidota
Caldisericota
Chloroflexota
Coprothermobacteriota
Cyanobacteria
Desulfobacteriota
Desulfobacteriota_B
Dormibacteriota
Eisenbacteria
Elusimicrobiota
Eremiobacteriota
Fibrobacteriota
Firmicutes_A
Firmicutes_B
Firmicutes_C
Gemmatimonadota
Halobacteriota
Krumholzibacteriota
Methanobacteriota
Methylomirabilota
Myxococcota
Nitrospirota
Patescibacteria
Planctomycetota
Proteobacteria (alpha)
Proteobacteria (gamma)
Spirochaetota
Thermoplasmatota
Thermoproteota
Verrucomicrobiota
WOR-3

883 **(Previous page) Suppl. Fig. S3 | Overview of the microbial diversity in Kilpisjärvi**
884 **soils based on a genome-resolved approach. a)** Number of metagenome-assembled
885 genomes (MAGs) shared between the different ecosystems. **b)** Number of detected MAGs across
886 the ecosystems. **c)** Relative abundance of the ten most abundant MAGs in each ecosystem,
887 computed as a proportion of reads mapping to each MAG. **d)** Metabolic potential of the MAGs
888 based on the annotation of genes against the KOfam database. Barplots represent the
889 proportion of MAGs in each phylum with complete pathways, i.e. containing ≥ 75% of the genes
890 in the pathway. Boxplots of carbohydrate-active enzymes (CAZymes) show the number of
891 different enzyme types identified in each MAG.

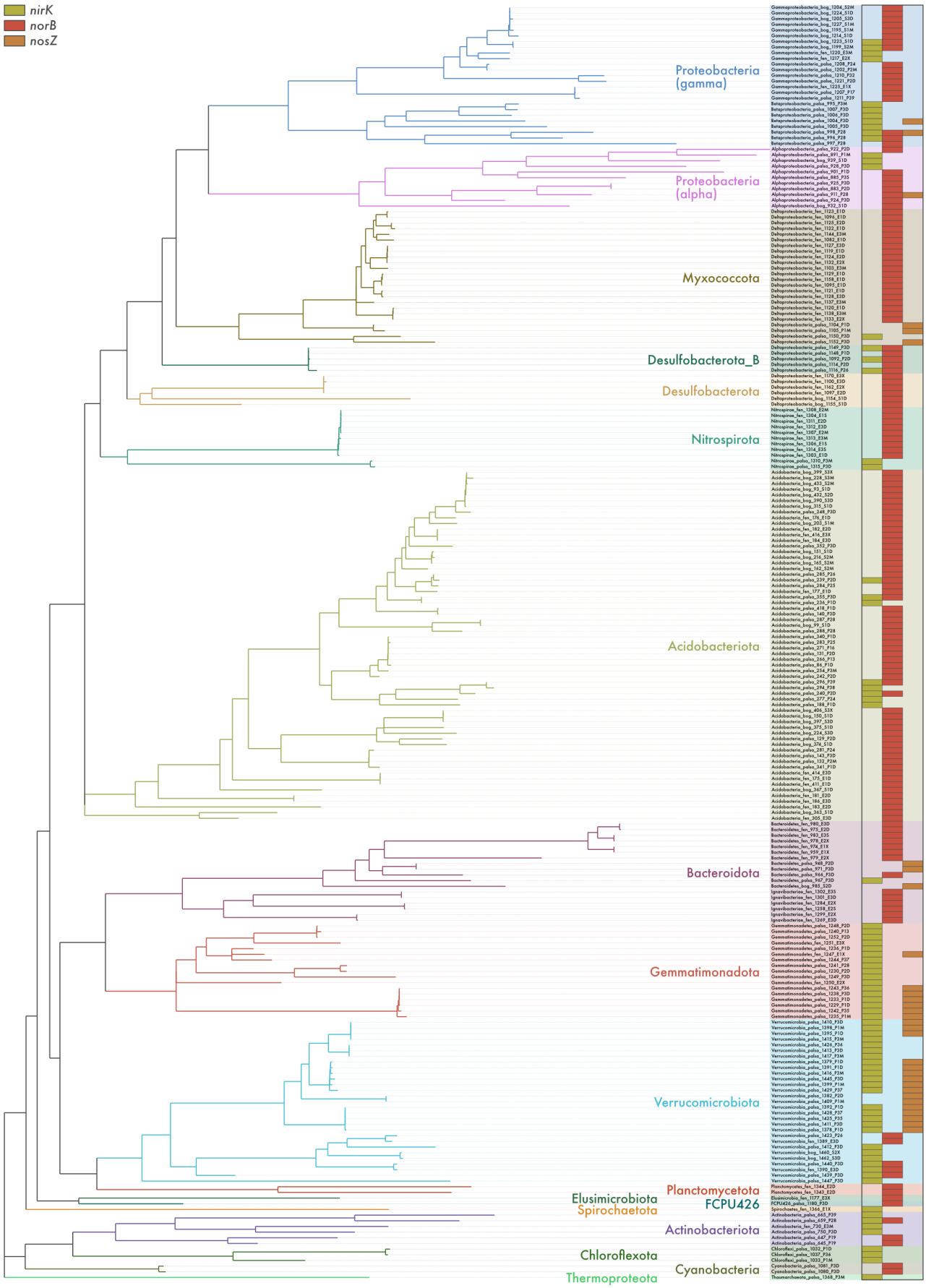
nirK
norB
nosZ
Proteobacteria (gamma)
Proteobacteria (alpha)
Myxococcota
Desulfobacterota_B
Desulfobacterota
Nitrospirota
Acidobacteriota
Bacteroidota
Gemmatimonadota
Verrucomicrobiota
Planctomycetota
Elusimicrobiota
FCPU426
Spirochaetota
Actinobacteriota
Chloroflexota
Cyanobacteria
Thermoproteota

892 **(Previous page) Suppl. Fig. S4 | Metabolic potential for denitrification in Stordalen**
893 **Mire soils.** Distribution of denitrification genes across 225 metagenome-assembled genomes
894 (MAGs) from permafrost peatland, bog, and fen soils in Stordalen Mire, northern Sweden. Genes
895 encoding the nitrite (*nirK*), nitric oxide (*norB*), and nitrous oxide (*nosZ*) reductases were
896 annotated using a three-step approach including (1) identification using hidden Markov models
897 from the KOfam database, (2) manual inspection for the presence of conserved residues at
898 positions associated with the binding of co-factors and active sites, and (3) phylogenetic analyses
899 along with sequences from archaeal and bacterial genomes. Phylogenomic analysis of MAGs
900 was done based on concatenated alignments of amino acid sequences from 122 archaeal and 120
901 bacterial single-copy genes.

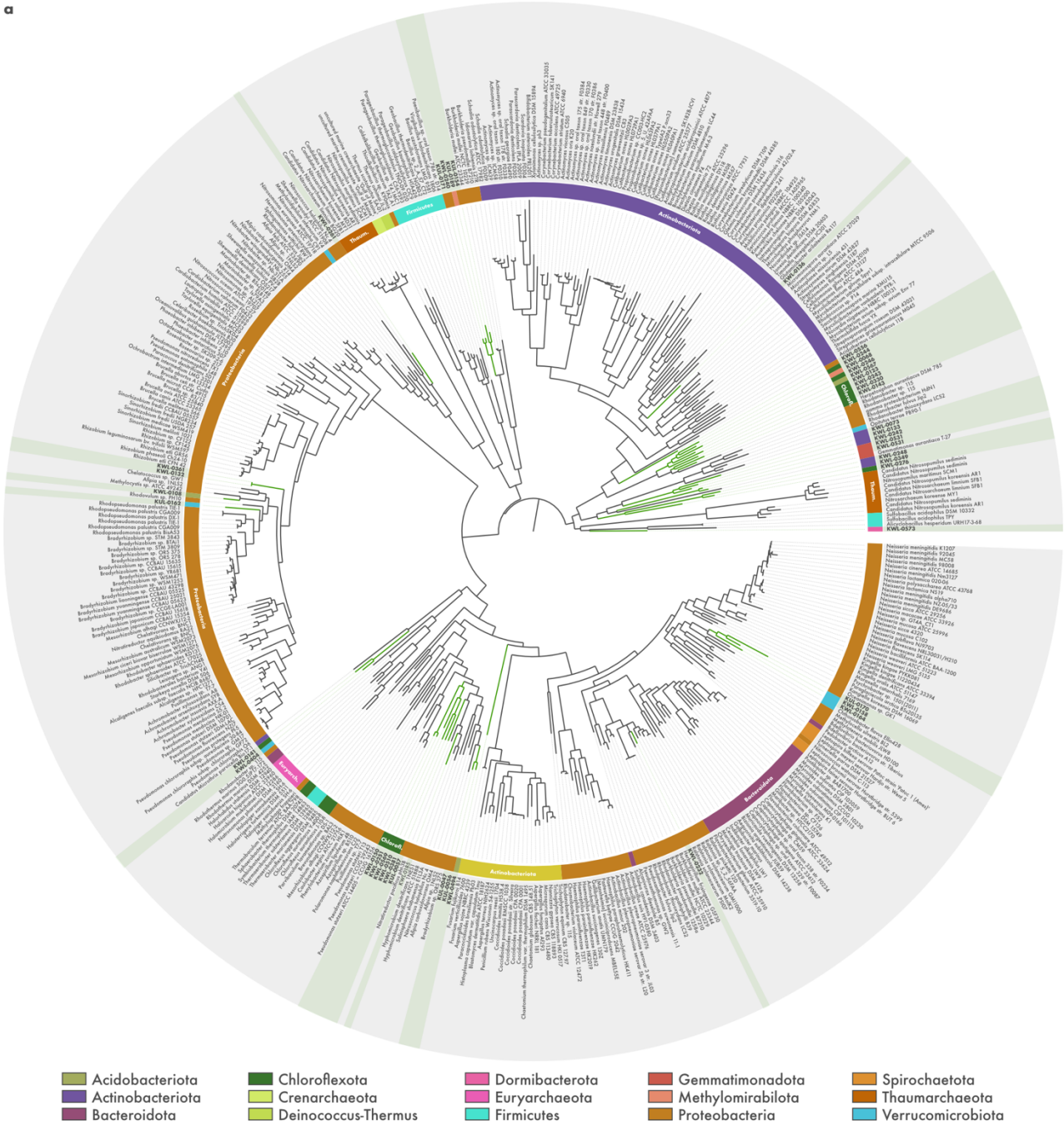

Suppl. Fig. S5 | Phylogeny of a) *nirK*, b) *nirS*, c) *norB*, and d) *nosZ* sequences from metagenome-assembled genomes (MAGs) recovered from tundra soils in Kilpisjärvi, northern Finland. Midpoint-rooted maximum-likelihood trees of translated sequences from Kilpisjärvi MAGs (highlighted) along with reference sequences from archaeal and bacterial genomes.

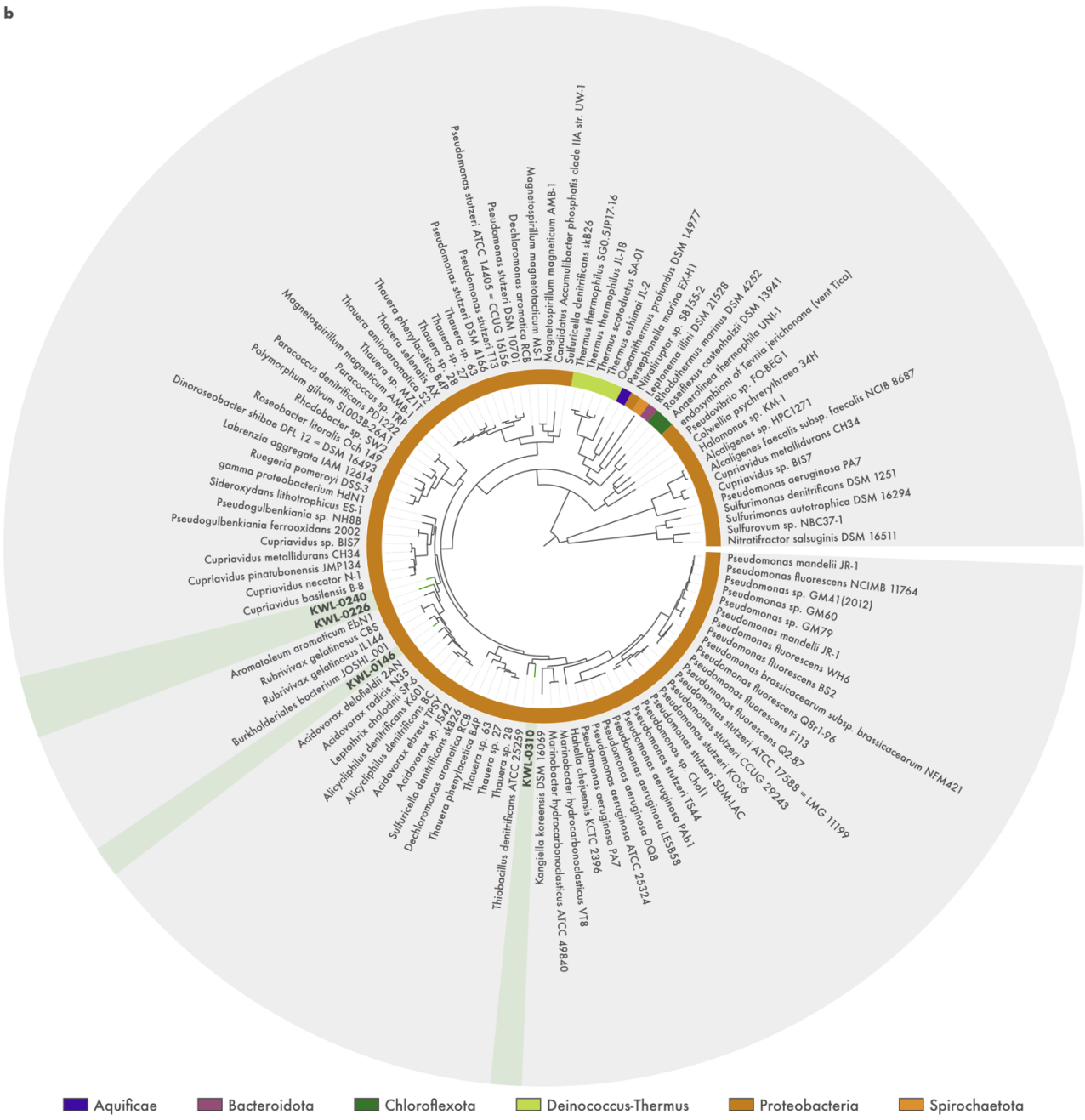
b
Candidatus Accumulibacter phosphatis clade IIA str. UW-1
Sulfuricella denitrificans skB26
Thermus thermophilus SG0.5JP17-16
Thermus thermophilus JL-18
Thermus scotoductus SA-01
Thermus ochrai JL-2
Oceanithermus profundus DSM 14977
Persephonella marina EX-H1
Nitratiruptor sp. SB155-2
Leptonema illini DSM 21528
Rhodothermus marinus DSM 4252
Roseiflexus castenholzii DSM 13941
Anaerolinea thermophila UNI-1
endosymbiont of Tevnia jerichonana (vent Tica)
Pseudovibrio sp. FO-BEG1
Colwellia psychrerythraea 34H
Halomonas sp. KM-1
Alcaligenes faecalis subsp. faecalis NCIB 8687
Alcaligenes faecalis CH34
Cupriavidus metallidurans CH34
Cupriavidus sp. BIS7
Pseudomonas aeruginosa PA7
Pseudomonas denitrificans DSM 1251
Sulfurimonas autotrophica DSM 16294
Sulfurimonas denitrificans
Sulfurovum sp. NBC37-1
Nitratifractor salsuginis DSM 16511
Pseudomonas mandelii JR-1
Pseudomonas fluorescens NCIMB 11764
Pseudomonas sp. GM41(2012)
Pseudomonas sp. GM60
Pseudomonas sp. GM79
Pseudomonas mandelii JR-1
Pseudomonas fluorescens WH6
Pseudomonas fluorescens BS2
Pseudomonas brassicacearum subsp. brassicacearum NFM421
Pseudomonas fluorescens Q8r1-96
Pseudomonas fluorescens F113
Pseudomonas fluorescens Q2-87
Pseudomonas stutzeri ATCC 17588 = LMG 11199
Pseudomonas stutzeri CCUG 29243
Pseudomonas stutzeri KOS6
Pseudomonas stutzeri SDM.LAC
Pseudomonas sp. Ch01
Pseudomonas stutzeri TS44
Pseudomonas aeruginosa PAb1
Pseudomonas aeruginosa LESB58
Pseudomonas aeruginosa DG8
Pseudomonas aeruginosa ATCC 25324
Pseudomonas aeruginosa PA7
Pseudomonas aeruginosa 2396
Hahella chejuensis KCTC 2396
Marinobacter hydrocarbonoclasticus VT8
Marinobacter hydrocarbonoclasticus ATCC 49840
Magnetospirillum magneticum AMB-1
Magnetospirillum magneticum MS-1
Magnetospirillum magnetotacticum MS-1
Dechloromonas aromatica RCB
Pseudomonas stutzeri DSM 10701
Pseudomonas stutzeri T13
Pseudomonas stutzeri ATCC 14405 = CCUG 16156
Pseudomonas stutzeri DSM 4166
Pseudomonas stutzeri ATCC 17588
Thauera sp. 63
Thauera sp. 27
Thauera sp. 28
Thauera sp. 29
Thauera sp. 63

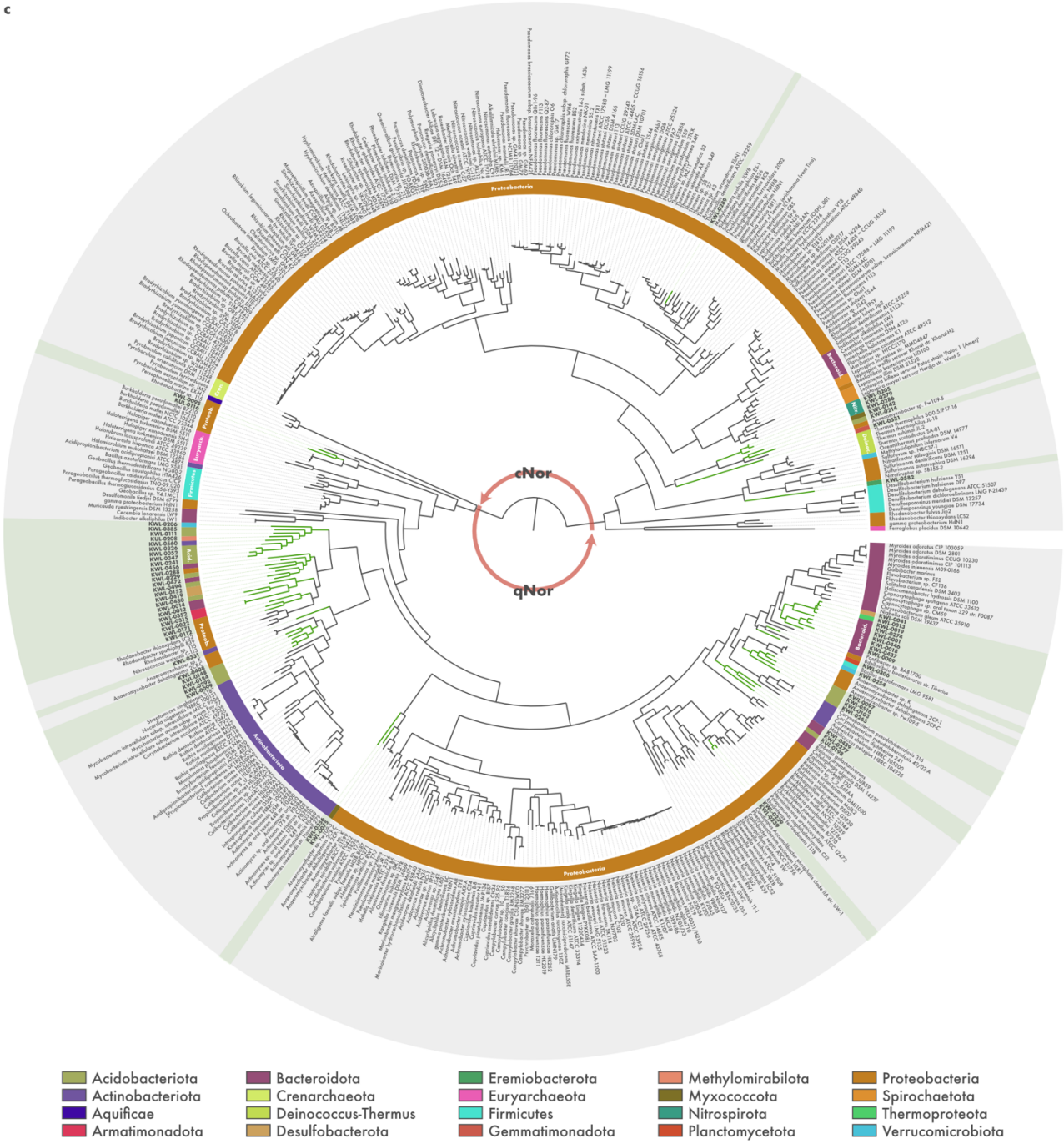

Suppl. Fig. S5 (continued) | Phylogeny of a) *nirK*, b) *nirS*, c) *norB*, and d) *nosZ* sequences from metagenome-assembled genomes (MAGs) recovered from tundra soils in Kilpisjärvi, northern Finland. Midpoint-rooted maximum-likelihood trees of translated sequences from Kilpisjärvi MAGs (highlighted) along with reference sequences from archaeal and bacterial genomes.

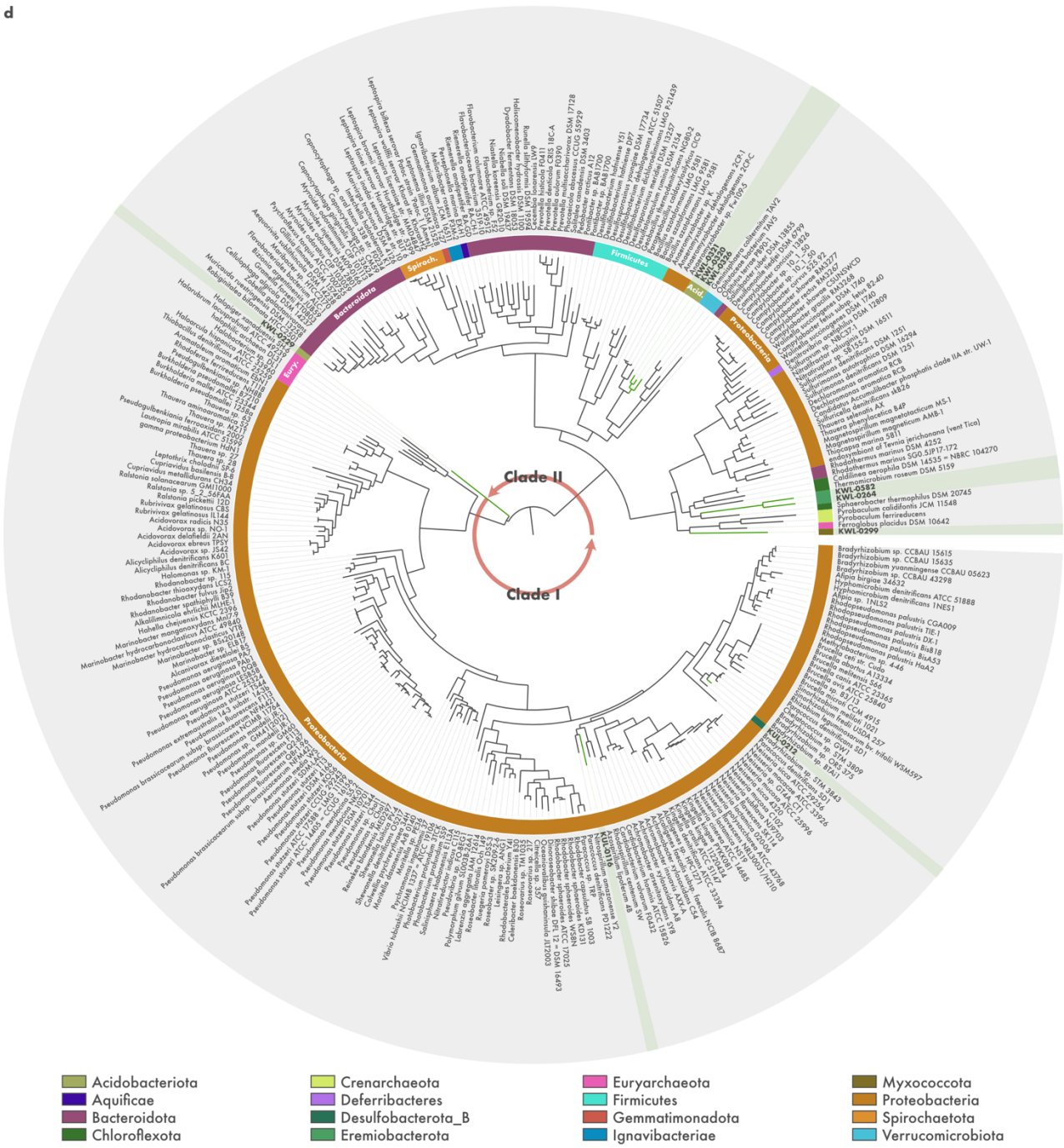

Suppl. Fig. S5 (continued) | Phylogeny of a) *nirK*, b) *nirS*, c) *norB*, and d) *nosZ* sequences from metagenome-assembled genomes (MAGs) recovered from tundra soils in Kilpisjärvi, northern Finland. Midpoint-rooted maximum-likelihood trees of translated sequences from Kilpisjärvi MAGs (highlighted) along with reference sequences from archaeal and bacterial genomes.

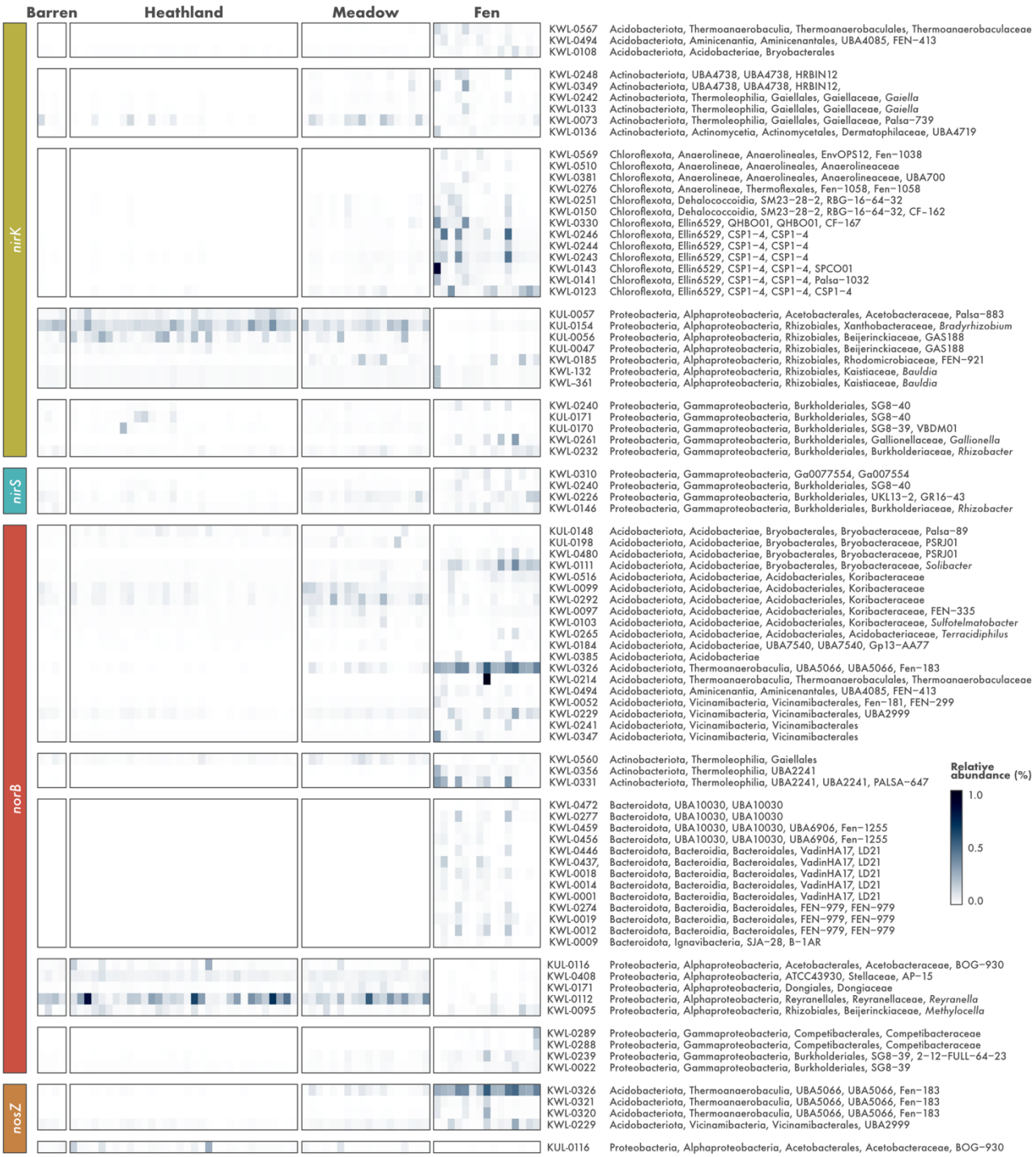

Suppl. Fig. S6 | Relative abundance of metagenome-assembled genomes (MAGs) harbouring denitrification genes across different soil ecosystems in the tundra. MAGs were recovered from soils in Kilpisjärvi, northern Finland, and annotated for genes encoding the nitrite (*nirK*/*nirS*), nitric oxide (*norB*), and nitrous oxide (*nosZ*) reductases using a three-step approach. Relative abundances were computed as a proportion of reads mapping to each MAG.